Parameters influencing moisture diffusion in epoxy-based materials during hygrothermal ageing-A review by statistical analysis

Camille Gillet, Ferhat Tamssaouet, Bouchra Hassoune-Rhabbour, Tatiana Tchalla, Valérie Nassiet

polymers

MDPI

Review

Parameters Influencing Moisture Diffusion in Epoxy-Based Materials during Hygrothermal Ageing—A Review by Statistical Analysis

Camille Gillet [1,2,*], Ferhat Tamssaouet [3], Bouchra Hassoune-Rhabbour [1], Tatiana Tchalla [2] and Valérie Nassiet [1,*]

[1] Laboratoire Génie de Production, INP-ENIT, Université de Toulouse, 47 Av. d'Azereix, 65000 Tarbes, France; bouchra.hassoune-rhabbour@enit.fr
[2] Safran Aircraft Engines, site de Villaroche, 77550 Moissy-Cramayel, France; tatiana.tchalla@safrangroup.com
[3] Laboratoire PROMES-CNRS (UPR 8521), Université de Perpignan, TECNOSUD, 66100 Perpignan, France; ferhat.tamssaouet@univ-perp.fr
* Correspondence: camille.gillet@enit.fr (C.G.); valerie.nassiet@enit.fr (V.N.)

Abstract: The hygrothermal ageing of epoxy resins and epoxy matrix composite materials has been studied many times in the literature. Models have been developed to represent the diffusion behaviour of the materials. For reversible diffusions, Fick, Dual–Fick and Carter *and* Kibler models are widely used. Many parameters, correlated or not, have been identified. The objectives of this review by statistical analysis are to confirm or infirm these correlations, to highlight other correlations if they exist, and to establish which are the most important to study. This study focuses on the parameters of the Fick, Dual–Fick and Carter *and* Kibler models. For this purpose, statistical analyses are performed on data extracted and calculated from individuals described in the literature. Box plot and PCA analyses were chosen. Differences are then noticeable according to the different qualitative parameters chosen in the study. Moreover, correlations, already observed in the literature for quantitative variables, are confirmed. On the other hand, differences appear which may suggest that the models used are inappropriate for certain materials.

Keywords: epoxy resin; composite material; hygrothermal ageing; water diffusion; Fick model deviation; statistical analysis; box plot; PCA

Citation: Gillet, C.; Tamssaouet, F.; Hassoune-Rhabbour, B.; Tchalla, T.; Nassiet, V. Parameters Influencing Moisture Diffusion in Epoxy-Based Materials during Hygrothermal Ageing—A Review by Statistical Analysis. *Polymers* **2022**, *14*, 2832. https://doi.org/10.3390/polym14142832

Academic Editors: Alexey Iordanskii and Alexandre Vetcher

Received: 19 June 2022
Accepted: 8 July 2022
Published: 12 July 2022

1. Introduction

For many decades, epoxy-matrix composites have been widely used in many industries, especially in aeronautics. Airframers seek to lighten the onboard aircraft mass as much as possible to reduce their fossil energy consumption. From that perspective, metals are substituted by polymer-matrix composite materials, which offer very high mechanical properties for a significantly lower density. Epoxy is a commonly used thermosetting polymer family, whether as a matrix in composite materials or as a structural adhesive for bonded joints and repairs in the aeronautical industry. Epoxy prepolymers and their hardeners form non-cross-linked systems with low viscosity, which ease their processing. They cover a wide range of cross-linking temperatures (from 5 to over 200 °C), depending on their chemical composition and the intended utilization. The epoxy system shrinkage after cross-linking is low compared to other thermosetting materials such as phenolic resins, making them good candidates as adhesives. In addition, the presence of polar functional groups such as hydroxyl gives them the ability to adhere to substrates or fibres. Besides, epoxies are commonly used as a matrix for composite materials because of their good mechanical properties and chemical resistance to many corrosive substances and acids. Epoxies also have good dielectric properties, allowing them to be electrical insulators [1,2].

However, despite their many beneficial properties, epoxy-based materials are sensitive to wet exposure as water molecules can penetrate their macromolecular networks. Water

molecule action can be reversible, as in the case of plasticization, or irreversible, such as hydrolysis. In the first case, the water molecules break the secondary bonds between neighbouring chains and partially destroy the mechanical cohesion of the polymer, which results in: (1) a decrease in the glass transition temperature T_g, which can be reversible; as well as (2) a loss of additives and the material swelling [3–5]. These swellings cause concentrations of mechanical stresses that can eventually lead to irreversible damage, such as decohesion between the fibre and the matrix or microcracks. Due to the difference in elasticity between the fibres and the matrix, and the water absorption, stresses develop along with the fibre/matrix interface. Within the sample, stress equilibrium is more easily maintained. However, at the surface, edge stresses are high enough to produce cracks. After cyclic exposure to a moist environment, micro-cracks and disbonds at the fibre/matrix interface tend to coalesce and expand [6–10]. In the case of hydrolysis, the water molecules penetrate directly to the macromolecule skeleton causing chain breaks, which destroy the cohesion of the material and allow the formation and propagation of cracks [11,12]. This decrease in mechanical properties is greatly impacting and has been widely demonstrated in the literature [13–21].

The literature has proved several times that hygrothermal ageing is governed by many parameters. These latter include, firstly: material parameters such as prepolymer type [22–25], hardener type [22,23,26], reinforcement type [13,27–29] or thickness [30,31]; secondly: conditioning parameters such as temperature [4,6,32] and relative humidity [22,33,34]; and thirdly: the resulting diffusion parameters such as saturation water mass uptake, saturation time and diffusivity [35]. Some of these parameters are correlated, meaning that they evolve together, while others are independent. The objective of this paper is to explore how these parameters influence each other and determine the principles behind this. Comparisons of water mass uptake by epoxy resin and epoxy-based composites have already been made in several publications, but without considering the variation of all the parameters [24]. A classical approach to comparing the different ageing mechanisms does not seem to be sufficient for a large dataset, because of the heterogeneity of the results.

This paper aims to confirm the correlations found by the literature between the different variables influencing the hygrothermal ageing and emphasize less apparent correlations. The objective is to highlight the most important variables of the problem, i.e., the most important to study.

Therefore, statistical studies on a large number of data were carried out. They include information on material type, ageing conditioning and parameters describing the diffusion curve. Data were extracted and calculated from *90 publications* on hygrothermal ageing of epoxy and epoxy-based composites: [4–7,10,13,15,16,18,19,22,24,26–34,36–104]. This study, which includes *448 individuals*, focuses on reversible gravimetric moisture uptake curves exhibiting Fick or Fick-derived two-step diffusion behaviour; water uptake is a function of the root of time. Irreversible behaviours, in particular those with mass losses during wet ageing or high mass uptake without asymptote, have been excluded from this study in order to avoid bringing together too different phenomena [22,32,105].

First, the diffusion parameters and the models to which they are related are presented. Then, the dataset is represented in order to study the relationships between the variables. For this purpose, box plots and scatter plots are generated to observe the variables' dispersion. However, the wide dispersion of the data could make it difficult to draw conclusions by simply observing the evolution of the variables between them. These data could present a great heterogeneity caused by the great diversity of the studied materials due to their different nature and process and the different conditioning parameters. All these parameters vary at the same time from one individual to another, which leads to different absorption behaviours, knowing that irreversible behaviours have already been ruled out. To complete the statistical study, the principal component analysis (PCA) is used. This analysis is effective for deducing correlations when a large number of quantitative variables is involved. By reducing and centering the variables, PCA facilitates observations despite their large dispersion. This includes:

- Highlighting material and ageing parameters influencing the diffusion parameters, by box plots and scatter plots;
- The correlation of the different quantitative parameters of the study by PCA;
- The separation of the data into four classified PCAs in order to propose more efficient correlations;
- Evidence of differences between PCA depending on the diffusion model and the type of material (resin or composite);
- Discussion of the limitations of using the diffusion models on epoxy-based materials.

2. Studied Parameters

The determination of diffusion parameters in the case of composites has been extensively study in the literature, with respect to the material configuration, the diffusion duration, and/or the diffusivity linearity, etc. [35,37,45,65,106–108].

Various models have been developed to describe the reversible behaviour of water absorption. The most well-known is the Fick model, for diffusion behaviour without anomaly, with a linear slope followed by saturation [109]. However, many epoxies show behaviours that deviates from the Fick model with the presence of two diffusion steps. Various models have been proposed to consider these anomalies, including the Dual–Fick model [20,110,111] and the Carter *and* Kibler model [19,21,45,51,112,113]. The equations of these three models are given below: Fick (Equation (1)), Dual–Fick (Equation (2)) and Carter *and* Kibler (Equation (3)).

$$M(t) = M_{sat}\left(1 - \frac{8}{\pi^2}\sum_{n=0}^{\infty}\frac{1}{(2n+1)^2}\cdot exp\left[-(2n+1)^2\cdot\pi^2\cdot\frac{D\cdot t}{h^2}\right]\right) \quad (1)$$

$$M(t) = \sum_{i=1}^{2}\left[M_{sat_i}\left(1 - \frac{8}{\pi^2}\sum_{n=0}^{\infty}\frac{1}{(2n+1)^2}\cdot exp\left[-(2n+1)^2\cdot\pi^2\cdot\frac{D_i\cdot t}{h^2}\right]\right)\right] \quad (2)$$

$$M(t) = M_{sat}\left(1 - \frac{8}{\pi^2}\sum_{l=1}^{\infty}\frac{r_l^+ exp(-r_l^- t) - r_l^- exp(-r_l^+ t)}{l^2(r_l^+ - r_l^-)} + \frac{8}{\pi^2}\frac{\kappa\beta}{l(\gamma+\beta)}\sum_{l=1}^{\infty}\frac{exp(-r_l^- t) - exp(-r_l^+ t)}{r_l^+ - r_l^-}\right). \quad (3)$$

In this study, the different parameters defining the diffusion are taken from those three models. For Fick behaviour individuals, the parameters selected are the saturation water mass uptake M_{sat}, the saturation time t_{sat} and the diffusivity D. Additional parameters are included to refine the observations for the two-step diffusion behaviour (abbreviated to Dual) individuals. Two parameters come from the Dual–Fick model: the water mass uptake at the first absorption step M_{inter}, and its time to be reached t_{inter} (Figure 1). The last three parameters, determined using the model developed by Carter *and* Kibler, that takes into account the functional groups of hydrophilicity, are: (1) γ the probability per time unit that free water molecules in the polymer will bond; (2) β the probability per time unit that bonded water molecules will liberate; and (3) K a parameter related to the material swelling. For the homogeneity purpose, all these parameters have been recalculated using the Carter *and* Kibler approximations, as a reminder [45]:

1- At the first step (intersection point between the two sorption stages):

$$\frac{M_{inter}}{M_{sat}} \cong \frac{\beta}{\gamma+\beta}; \quad (4)$$

2- At short times (curve linear domain):

$$\frac{M_{inter}}{M_{sat}} = \frac{4}{\pi^{3/2}}\left(\frac{\beta}{\gamma+\beta}\right)\sqrt{Kt}; \quad (5)$$

3- At longer times (beyond the first step):

$$\frac{M(t)}{M_{sat}} \cong \left\{1 - \frac{\gamma}{\gamma + \beta}(e^{-\beta t})\right\}; \quad (6)$$

where: $K = \frac{\pi^2 D}{2h^2}$, D is the diffusivity, and h is the sample thickness.

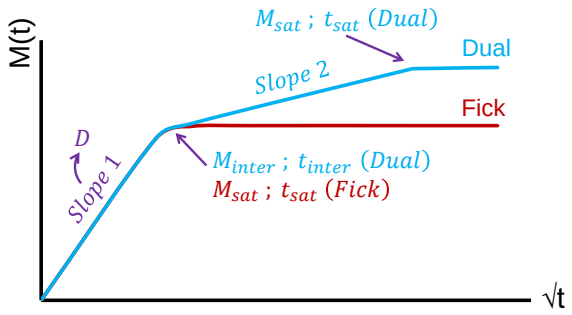

Figure 1. Fick and two-step (Dual) diffusion curves, positions of M_{sat}, t_{sat}, M_{inter} and t_{inter}.

All these parameters are related to the material parameters: prepolymer type, hardener type, reinforcement type, fibre architecture, fibre volume fraction v_f, thickness h, process; and conditioning parameters: conditioning (immersion in water or exposure to humid air), relative humidity RH, and ageing temperature T_{ageing}. Some variables are qualitative while others are quantitative (Table 1).

Table 1. List of variables used for the dispersion study.

	Material Parameters	**Ageing Parameters**	**Diffusion Parameters**
Qualitative	Prepolymer type Hardener type Reinforcement type Fibre architecture Process	Conditioning	Diffusion behaviour
Quantitative	v_f h	RH T_{ageing}	D M_{sat} t_{sat}

3. Descriptive Statistics: Study of Dispersion

To observe the variables' dispersion and study their mutual influence, the whole dataset is represented using box plots. This allows the removal of outliers and the highlighting of the median and central quartile values. As a result, the dataset is separated into four equally sized portions. Each of the three values that divide the elements of a statistical distribution is called a quartile. The box contains 50% of the individuals: 25% between the first quartile and the second quartile-or median-and 25% between the median and the third quartile. The "whiskers" are the lines that run across the box. They indicate the variability outside the quartiles, and each includes 25% of the individuals. The points outside the whiskers are atypical values.

With this first scatter analysis, the entire dataset is observed. The dispersion of the quantitative values saturation mass uptake M_{sat}, diffusivity D and saturation time scaled to thickness t_{sat}/h are studied, as a function of the categorical variables that describe the dataset: diffusion behaviour, prepolymer type, hardener type, reinforcement type, fibre architecture, process, and conditioning (Table 1). Time was reduced to thickness to normalize the results and obtain comparable durations. These three quantitative variables were also observed as a function of other quantitative variables: fibre volume fraction, relative humidity rate RH, and ageing temperature T_{ageing}. For this purpose, scatter plots were generated.

The *R* programming language and software, its packages *corrplot* and *factoextra*, as well as the *boxplot* function are used [114–116].

3.1. Diffusion Behaviour

The two types of moisture diffusion behaviour, Fick and Dual diffusions, are studied. Figure 2 shows the data distribution within quartiles for the variables t_{sat}/h, D and M_{sat}. All characteristic values of the box plots are shown. Outliers are not shown for the sake of clarity, but their percentage is indicated. One can observe that the distributions are not centered, and all the variables and behaviours have a higher skewness, which shows that they are not normal (Gaussian). This is reflected in the fact that some individuals have higher mass absorption, longer saturation time, and greater diffusivity, i.e., greater sensitivity to moisture. The box plot shows that the same median is obtained regardless of the moisture diffusion behaviour. In contrast, the third quartile and the upper whisker boundary are larger for specimens with two diffusion steps. As many individuals are located on either side of the median, but beyond this median, they are more widely spaced, and some have a large diffusivity that stretches the graph. Diffusivity and saturation time reduced to thickness reveal a very wide dispersion from one behaviour to another. For t_{sat}/h, the gap between the two behaviour types is around 10^2 for the median, which is very large.

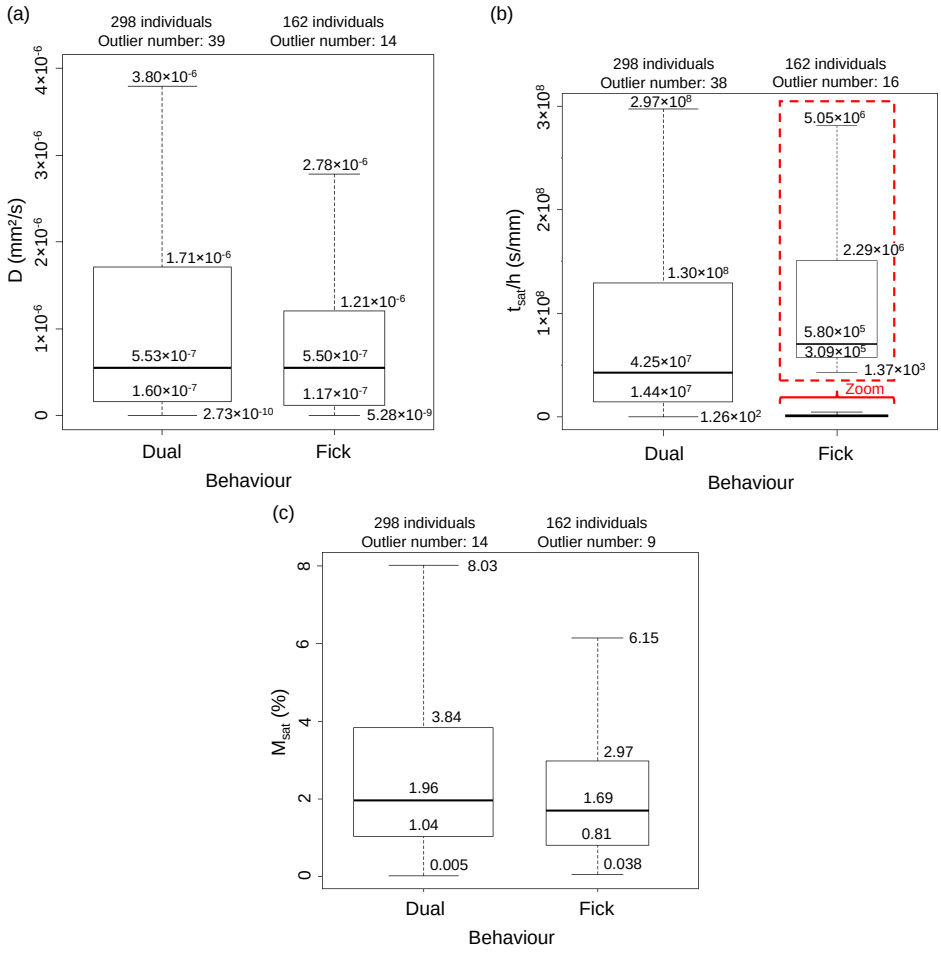

Figure 2. Box plots and characteristic values of (**a**) D, (**b**) t_{sat}/h and (**c**) M_{sat} as a function of the diffusion behaviour.

For the saturation mass uptake, the median is slightly lower for Fick individuals than for individuals with two diffusion steps. For Fick individuals, the distance between quartiles is similar. A low dispersion of epoxies and epoxy-based composites is observed.

Indeed, in this study, 75% of the individuals have a moisture absorption lower than 4%. The diffusivity and the saturation time show strong dispersion. While saturation can take considerable time, the saturation mass uptake varies only slightly after passing the first diffusion step. These differences in diffusion behaviour depend on the different parameters given in the Table 1. Indeed, the diffusion parameters differ according to the material parameters and the ageing parameters, detailed in the following.

3.2. Epoxy Prepolymer Type

Some polymers are more likely to absorb water due to their hydrophilicity [102,117–119], or the free volume presence [120–122]. Among the epoxy family, differences were found in the prepolymers functional groups and in their structure. The dataset is sorted according to the prepolymer type in order to observe the variation in the dispersion of M_{sat}, t_{sat}/h and D. For the sake of simplicity, only medians are shown (Table 2) and the entire box plots are available as Supplementary Materials (Figures S1–S3). Medians divide the studied populations into two sets comprising the same number of individuals. One can notice that these individuals show high skewness similarly to the box plots based on diffusion behaviour. Looking at the saturation mass uptake, we find values about 1.05% for the DGEBF resin and 6.37% for the DGEBA + novolac resin. In contrast, the DGEBA and novolac resins have weaker saturation mass uptake when unblended. The other blends (DGEBA + mTGAP, DGEBA + TGDDM) also appear to have lower moisture absorption than the neat resins. Furthermore, the mTGAP resins also show strong moisture absorption, which can be explained by the fact that they are two aromatic epoxy prepolymers with three oxirane groups and a nitrogen atom, which are very hydrophilic [25,117,118,123,124].

Table 2. Medians of M_{sat}, t_{sat}/h et D as a function of epoxy prepolymer type. List of pre-polymers and entire box plots are available as Supplementary Materials (Figures S1 and S3–S5).

Name (Individuals Number)	M_{sat} (%)	t_{sat}/h (s/mm $\times$ 10^7)	D (mm^2/s $\times$ 10^{-7})
DGEBA based (217)	1.61	0.80	5.23
DGEBA + mTGAP (3)	4.44	0.16	106
DGEBA + novolac (3)	6.37	22.30	0.50
DGEBA + TGDDM (2)	4.31	4.96	13.00
DGEBD (5)	6.15	0.02	17.40
DGEBF based (15)	1.05	7.02	3.49
ESO (11)	1.75	0.18	4.67
mTGAP (7)	5.35	0.16	56.61
Novolac (11)	2.26	0.36	15.50
Rubber-modified epoxy (2)	3.08	8.02	0.47
TCDAM (1)	3.84	8.02	0.47
TGDDM (80)	1.50	2.26	4.36
TGDDM + mTGAP (14)	2.02	1.71	6.62
Unknown epoxy (89)	2.64	1.69	9.07

Indeed, the hydrophilicity of the polymer is linked to the nature of the chemical groups composing the macromolecules. Water molecules are attracted to polar functions, such as hydroxyls or nitrogens. According to Van Krevelen, water absorption is an additive molar function. For a representative structural unit, independent of its environment, it is written (Equation (7)) [117,118]:

$$H = \frac{M(t) \cdot M}{1800}, \tag{7}$$

where H is the number of water moles, M is the molar mass and $M(t)$ is the percentage of mass uptake. There are universal values of H. For non-polar hydrocarbons (–CH–, –CH_2–, –CH_3), fluorinated groups or aromatic rings: $H = 0$. Moderately polar groups, such as esters and ethers, have $H < 0.3$. Hydrogen bonding groups, e.g., acids, alcohols, amides, amines and hydroxyls, are very hydrophilic and have: $H = 1$–2 [25,118,123–125]. Some structures combine hydrophilic and hydrophobic groups, such as polyamides and

epoxies. The hydrophilicity then depends on the respective proportions of these groups. These predictions apply in the case where the contributions of the different groups are independent. For epoxies, where internal hydrogen bonds can interact with hydrogen bonds caused by moisture uptake, it is necessary to consider structural units that include groups interacting with each other [101,102,119,126].

However, the TGDDM prepolymers, composed of four oxirane groups and two nitrogen atoms, do not experience such large moisture absorption. Another phenomenon that affects moisture uptake is the gelation rate. Indeed, faster gelling traps more voids and has a lower cross-linking density. For example, Frank et al. report this to be the case for mTGAP/DDS, which has a greater saturation mass uptake than DGEBA/DDS. Nevertheless, the size of the free volumes decreases with the macromolecule functionality because of the increase of the cross-linking density. So although TGDDM/DDS has four functionalities against three for mTGAP/DDS, its longer and more flexible skeleton allows it to have smaller free volumes and lower absorption [41,44,119].

Different profiles are observed in Table 2. The highest absorption rates are not always associated with large diffusivities or long saturation times. The more polar functions the epoxy has, the greater the diffusion temperature dependence and the more hydrophilic it is. In this study, a pretty low saturation mass uptake is associated with a high saturation time and a low diffusivity, and vice versa: for example, DGEBF, ESO, TGDDM or DGEBA resins. On the other hand, not all specimens respect this behaviour as the DGEBA + Novolac mixtures and mTGAP combine low diffusivities, long saturation time and high saturation mass uptake. The diffusion depends on the absorption curve shape. According to [25], polar sites in hydrophilic systems could act as a barrier to diffusion. Polar groups act as "bottlenecks" and trap incoming water molecules, named bonded water, which inhibits their free diffusion within the free volumes. Considering the data dispersion, the curing effect on moisture sensitivity should also be taken into account. Indeed, Abdelkader and White find that imperfect resin cross-linking leaves uncrosslinked epoxy areas that are more sensitive to water and enable faster penetration into the material. In addition, cross-linking at excessive temperatures could reduce the polymer density through the porosities formation. These porosities allow water molecules to have more free volumes in which to settle [26,102].

3.3. Hardener Type

Due to the large number of hardener types, they are classified according to their chemistry: amine, amidoamine, dicyandiamide, anhydrid acid and phenol novolac. Since 276 individuals are amine, or 62%, this category of hardeners was divided into four, according to their structure: aliphatic, cycloaliphatic, aromatic and unknown when not given in the publication (Table 3).

Table 3. Medians of M_{sat}, t_{sat}/h and D as a function of the hardener type. List of hardeners and entire box plots are available as Supplementary Materials (Figures S2 and S6–S8).

Name (Individuals Number)	M_{sat} (%)	t_{sat}/h (s/mm $\times 10^7$)	D (mm^2/s $\times 10^{-7}$)
Aliphatic amine (51)	2.61	1.23	8.51
Aromatic amine (139)	2.63	1.62	5.79
Cycloaliphatic amine (14)	1.81	4.32	3.15
Amidoamine (16)	1.47	0.44	9.18
Dicyandiamide (61)	1.59	5.24	3.46
Anhydride acid (42)	1.01	0.87	4.42
Phenol Novolac (9)	2.10	0.36	5.56
Unknown amine (71)	0.79	0.28	7.33
Unknown hardener (57)	3.20	2.92	8.57

The classification by the type of hardener in this paper shows a lower dispersion than the classification by the type of prepolymer, for example, medians of the saturation mass uptake range from 0.79% to 3.20%. It should be taken into account that the crosslinking

sites of thermoset materials are generally considered hydrophilic due to the high presence of hydrogen bridges, which tend to absorb more water [127–129]. For example, polyvinyl alcohol, polyacrylamides, amine and amide hardeners are very hydrophilic, which may explain this lower dispersion.

In the box plots, both aliphatic and aromatic amines show similar saturation mass uptake and saturation time medians. The diffusivity is lower for the aromatics. Cycloaliphatic amines have slightly lower saturation mass uptake, significantly lower diffusivity medians and longer saturation times. The unknown amines have much lower M_{sat} and t_{sat}/h, but D close to those of aliphatic amines. This result conflicts with some observations in the literature, where aliphatic amines have higher saturation masses than aromatic amines [26,41]. Amidoamines have much lower M_{sat} and t_{sat}/h than aliphatic, aromatic and cycloaliphatic amines. On the other hand, they show the highest D medians of the study. The dicyandiamides have the highest t_{sat}/h medians. The anhydrid acids have low M_{sat} and t_{sat}/h. Phenol novolacs exhibit low t_{sat}/h, with M_{sat} and D close to those of aromatic amines.

Hardeners with a bulky structure, such as amidoamines, enable us to obtain a flexible network because of their long macromolecules with a high functionality. The steric hindrance is very important, which causes significant free volume, allowing the rapid entrance of water molecules [26]. On the other hand, their chemistry does not present more hydrophilic sites than other types of hardeners, such as amines, which can explain the rather low M_{sat} medians. For aromatic amines, such as dianilines, the variation in their sensitivity to moisture is related to their reactivity and polarity. Furthermore, the hydroxyl and tertiary amine groups play a concerted role in the water bonding to the network, making their group contributions indistinguishable. The formation of a water-amine hydrogen bond competes directly or indirectly with an internal hydroxylamine hydrogen bond whose strength increases with the amine nucleophilicity. The indirect effect would occur if the water placement required a site of a particular steric configuration which, in its turn, depends on the amine-hydroxyl interaction [26,119].

Among the cycloaliphatic amines, many are IPDA, which are quite hydrophobic due to their CH_3 groups. These results have already been observed in the literature. The aliphatic and aromatic amines are all moderately hydrophilic due to their chemical composition. The most important saturation M_{sat} are linked to relatively low t_{sat}/h compared to the others. This may also apply to anhydride acid. In this hardener family, we observe hydrophobic specimens due to the CH_3 presence, which reduces their hydrophilicity. This may be the case with acetic anhydride. However, they are also more sensitive to humidity anhydrides, such as methylhexahydrophthalic anhydride (MHHPA). Epoxy anhydrides subjected to absorption followed by hydrolysis-related mass losses have been reported in the literature [22]. Hydrolysis-sensitive hardeners, such as some anhydrides or dicyandiamides, could then have lower mass uptakes.

3.4. Fibres Presence

While epoxy resin matrices are subject to wet ageing, carbon fibres can be considered impervious to moisture. Similarly, glass fibres are considered to have a low sensitivity to moisture over the material lifetime. It is important to note that despite their impermeability, these inorganic fibres impact moisture diffusion as they modify the behaviour of the polymer at the fibre-matrix interface. Differential swelling occurs and develops high stresses. Decohesion occurs if the adhesion is not sufficient. A void then appears at the interface, and the water uses it to propagate more rapidly through the material, like a moisture carrier [8,39,118]. In the study, composites based on carbon and glass fibres have the lowest median absorbed water mass uptake, with 1.39% for carbon and 0.80% for glass (Table 4). Their median diffusivities and saturation times are also the lowest among all the reinforcement types. As glass and carbon fibres are not very sensitive to water, M_{sat} should be reduced to the resin mass fraction in order to take into consideration only the matrix part in the composites. We also note that the M_{sat} and D box plots for the glass fibres are centred, i.e., the specimens are homogeneously distributed on either side of the medians, which is equal to the mean, despite the differences in resin type and conditioning. This

low dispersion of values may be due to the diffusion inertia associated with the presence of fibres.

Table 4. Medians of M_{sat}, t_{sat}/h and D as a function of the reinforcement type. "None" refers to a neat resin, without reinforcement. Entire box plots are available as Supplementary Materials (Figures S9–S11).

Name (Individuals Number)	M_{sat} (%)	t_{sat}/h (s/mm $\times 10^7$)	D (mm^2/s $\times 10^{-7}$)
Aramid (30)	3.54	1.16	6.90
Carbon (127)	1.39	1.53	3.64
Flax (7)	9.82	0.60	14.20
Glass (88)	0.80	0.69	3.63
Hemp (6)	13.0	4.14	9.18
Hybrid carbon aramid (1)	1.62	1.30	3.52
Hybrid carbon glass (7)	3.33	0.04	25.92
Regenerated cellulose (2)	7.10	6.98	13.91
None (192)	2.87	1.59	6.54

The box plots highlight the flax, hemp and regenerated cellulose fibre composites, which have median saturation masses of 9.82, 13.0 and 7.10%, respectively. Their median diffusivity is slightly higher than the other materials. Thus, for the hemp and regenerated cellulose fibre individuals, the median saturation times is also higher. It is recognized in the literature that these organic vegetal fibres are sensitive to water. This sensitivity depends on their chemical composition, in particular on their lignin and hemicellulose content [130]. In the composite, in addition to the matrix, the fibres also absorb moisture. Indeed, organic fibres are subject to swelling, which can cause matrix cracking and accelerated water diffusion, resulting in a higher mass of absorbed water than in the neat resin [3,9,89]. Surface treatments can then be used on organic fibres to reduce their hydrophilicity and the moisture absorption they induce. For example, potassium hydroxide and sodium hydroxide are used to reduce the ability to create hydrogen bonds between natural fibres and water. For cellulose fibres, they will remove open hydroxyl groups. Silane can also be used to stabilize the fibres and make them resistant to leaching by masking hydroxyl groups, by creating silanol, and reducing the number of porosities [131–133]. Aramid fibres are also organic fibres, composed of very hydrophilic amide bonds, but they do not seem to cause disproportionate moisture absorption, with a median saturation mass uptake of 3.54%.

A composite material can have different behaviours on which the diffusion properties depend. The fibres' presence initially leads to a change in the flow path of water molecules, creating anisotropic diffusion at the macroscopic scale, which is the composite scale. Zhou and Lucas studied the dimensional changes that can be caused by the presence of fibres on carbon/epoxy composites immersed in distilled water at different temperatures. The diffusion along the fibre shows extreme stability, and no dimensional changes were measured. This stability is due to the carbon fibres high longitudinal stiffness. As they are impermeable to water absorption, the longitudinal dimension of the fibre is considered invariant. In width, the fibres hold and block the matrix, which prevents peeling. However, in the thickness, there are layers of neat epoxy that are not blocked by the fibres, which can peel under severe ageing. If saturation is reached, there is no longer any dimensional change [7]. The water diffusion in the composite material is strongly dependent on the fibre volume fraction v_f, and their arrangement, which affects both the gap size between two fibres and the diffusion path length through the matrix [35,110,112,134]. The effect of fibre volume fraction on moisture diffusion is complex, as the statistical study shows in Figure 3. M_{sat}, t_{sat}/h and D they show an increase as a function of v_f up to a certain threshold beyond which they fall. The fewer the gaps between the fibres, the shorter the diffusion paths through the matrix. As the fibre volume fraction increases, the diffusivity increases. However, if it is too important, the fibres are grouped and can touch each other.

In this situation, the local diffusion is blocked and therefore is very low [33,112,134]. In Figure 3, the evolution of the variables seems to be in accordance with these conclusions.

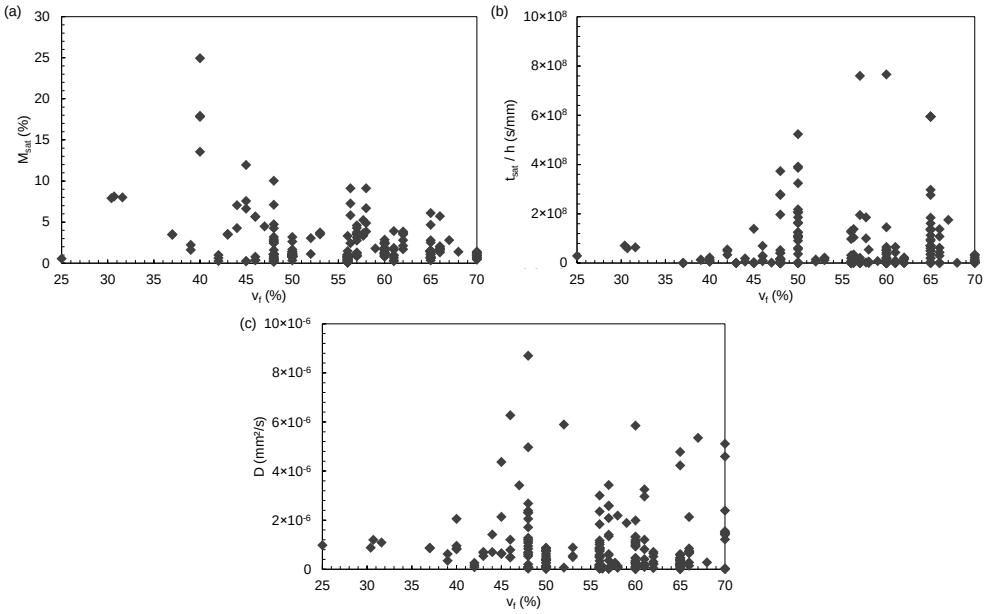

Figure 3. Evolution of (**a**) M_{sat}, (**b**) t_{sat}/h and (**c**) D as a function of the fibre volume fraction v_f.

Observing the reinforcement architectures used in the dataset, the composites composed of long fibre mats have a very important median absorbed mass uptake, which can be explained by the large voids created during its manufacture process (Table 5). This median absorbed mass uptake is quite similar for reinforcements arranged in one direction (UD), in two directions (2D), balanced, or in three dimensions (3D). It is slightly higher for UD and balanced reinforcements than for 3D. The median diffusivities are the greatest for the balanced and 3D composites, and the median saturation times are also the shortest for these two reinforcement configurations. The water molecules may have more directions to propagate, and and saturation is reached more rapidly. The literature is not uniform on this issue. Tang et al. found by modelling that their balanced woven fabrics diffused faster than their UD, particularly when the fibre waviness was greater [134]. For Yuan et al., the experimental data and modelling reveal a greater water mass absorbed in their 3D than in their UD. They also report a higher bound water proportion throughout the material [95]. On the other hand, Almudaihesh et al. observe that their UD composites absorb more water than their woven composites [135]. Finally, Wan et al. obtained a lower saturation mass uptake and diffusivity for their 3D than their UD. Their suggestion is that the moisture diffusion path is distorted in the 3D, which exerts a greater hindrance than for the UD [136].

Table 5. Medians of M_{sat}, t_{sat}/h and D as a function of architecture reinforcement. Entire box plots are available as Supplementary Materials (Figures S12–S14). UD: one direction, 2D: two directions, 3D: three dimensions.

Name (Individuals Number)	M_{sat} (%)	t_{sat}/h (s/mm $\times$ 10^7)	D (mm^2/s $\times$ 10^{-7})
UD (93)	1.50	1.73	3.49
2D (94)	0.95	1.51	3.99
Balanced (47)	1.80	0.12	8.68
3D (5)	0.99	1.30	6.25
Long Fibre mat (4)	17.87	1.88	9.05
Unknown (2)	2.64	3.21	4.69

3.5. Manufacturing Process

Many processes have been developed to manufacture polymer or organic matrix composite materials. The process choice depends on various criteria: production speed, cost, desired performance, size and shape, resin and fibres nature. The quality of the process affects its cross-linking rate and the porosity percentage. Manufacturing processes applying pressure, such as resin transfer moulding (RTM), thermopressing or prepreg curing in the autoclave, result in a high fibre volume fraction and low porosity [136–138]. With these processes, the median saturation mass uptakes, saturation times and diffusivities appear relatively low. The dispersion of these values is also small (Table 6).

Table 6. Medians of M_{sat}, t_{sat}/h and D as a function of the process. Entire box plots are available as Supplementary Materials (Figures S15–S17).

Name (Individuals Number)	M_{sat} (%)	t_{sat}/h (s/mm $\times 10^7$)	D (mm^2/s $\times 10^{-7}$)
Autoclave (98)	1.52	6.36	3.48
Contact moulding (9)	3.41	2.07	36.60
Filament winding (2)	2.28	66.20	5.52
Heating table (9)	3.33	0.03	21.9
Infusion (28)	1.81	1.48	8.65
Moulding (195)	2.81	1.13	7.00
Pultrusion (1)	2.80	17.5	53.5
RTM (31)	0.89	0.89	7.90
Thermopressing (24)	2.70	2.86	9.48
Unknown (63)	0.94	0.32	1.71

Contact moulding and heating table processes show high median diffusivity and mass uptake. These processes have the common feature that they do not use pressure. They do not allow for high volume fractions of fibres. In addition, the fibres distribution and the resin content are not uniform, which can lead to voids formation. They show a noticeable data dispersion, probably because the dispersion and the quantity of porosities are variable, depending on the manufacturing parameters used.

Infusion, which has intermediate water absorption properties, also shows quite a large data dispersion. The vacuum bag low compaction is the cause of a greater void formation compared to other pressurized processes such as autoclave, which is responsible for greater diffusion and moisture absorption. Nevertheless, it is possible to improve the polymer quality by influencing its viscosity. A high viscosity may be responsible for a higher porosity. This porosity, therefore, varies according to the chosen resin type and cross-linking parameters, which may explain the wide dispersion of the data [139,140].

Concerning the unknown manufacturing process materials, it may be interesting to specify that these are generally aeronautical composites for which the information has not been revealed in the source publication. They may therefore be materials with high properties, which explains their low saturation mass uptakes and diffusivities.

3.6. Ageing Conditions

3.6.1. Conditioning Environment

Wet ageing can occur at various locations: in water, whether distilled water, seawater or deionised water, or in the humid air. In the literature, these environments have been widely studied. In addition, deionised water and humid inert atmosphere are also analyzed. By examining the individuals immersed in water, a similar median saturation mass uptake appears for distilled and deionised water, while it is much lower for seawater. Although the box plots for distilled water are almost centred, indicating good results homogeneity, the box plots for deionised water are eccentric towards the top (Table 7). The lowest saturation mass uptakes are obtained under humid air, while the highest are obtained in immersion in distilled or deionised water. Mass uptakes in seawater is also low. The mineral presence in the water slows down the water molecule diffusion through the material and leads

to lower saturation masses, although these differences are mainly perceived over long ageing times [12,47,64]. In contrast, diffusivity under humid air is much higher and allows saturation to be reached most quickly. It is followed by the diffusivity under distilled water, which is very close. Finally, the diffusivity in deionised water appears to be the lowest, despite the absence of minerals that could slow down the water molecule diffusion. Nevertheless, in the database, the number of individuals immersed in deionised water or seawater is very low compared to the number of individuals immersed in distilled water, which could be linked to this divergence of results. It is possible that other parameters have a greater influence on the values of M_{sat}, t_{sat}/h and D than the water type.

Table 7. Medians of M_{sat}, t_{sat}/h and D as a function of the conditioning environment. Entire box plots are available as Supplementary Materials (Figures S18–S20).

Name (Individuals Number)	M_{sat} (%)	t_{sat}/h (s/mm $\times 10^7$)	D (mm^2/s $\times 10^{-7}$)
Humid air (215)	1.08	0.57	5.90
Inert atmosphere (2)	2.03	3.88	24.4
Deionised water (20)	3.09	0.89	0.95
Distilled water (203)	3.12	1.99	5.79
Sea water (20)	1.43	2.77	3.50

3.6.2. Relative Humidity

The relative humidity percentage influence on the absorbed water mass by epoxy-based materials has been demonstrated many times in the literature and is no longer in doubt [18,45,51,53–55]. This statistical study confirms that the higher the relative humidity, the greater the saturation mass uptake M_{sat} (Figure 4). Immersion of this material type in distilled water further increases its absorbed water mass [22].

This dataset effectively confirms the positive correlation between the absorbed water mass uptake and the relative humidity. Henry's law allows this correlation to be represented for humid air conditioning (Equation (8)) [20,124].

$$C_{sat} = SP_s, \tag{8}$$

where C_{sat} is the saturation water concentration and P_s is the water partial pressure, linked with RH (Equation (9)).

$$RH(\%) = 100\frac{P_s}{P_{sat}}. \tag{9}$$

Several versions of this law adapted to Dual sorption were subsequently developed: power law (Equation (10)) [37]; Langmuir (Equation (11)) [141]; Dual sorption (Equation (12)) [142]; and Flory–Huggins (Equation (13)) [143].

$$C_{sat} = a\left(\frac{P_s}{P_{sat}}\right)^b \tag{10}$$

$$C_{sat} = \frac{cP_s}{1 + dP_s} \tag{11}$$

$$C_{sat} = SP_s + \frac{cP_s}{1 + dP_s} \tag{12}$$

$$\ln a_s = \ln\frac{P}{P_s} = \ln v + (1 - v) + \chi(1 - v)^2, \tag{13}$$

with a, b, c and d as coefficients, a_s the solvent activity, v the volume, and χ the polymer-solvent interaction coefficient. For pure resins, b is between 1.3 and 1.8 while it is close to 1 for composite materials. c and d are given approximately by the statistical thermodynamic treatment of Langmuir's.

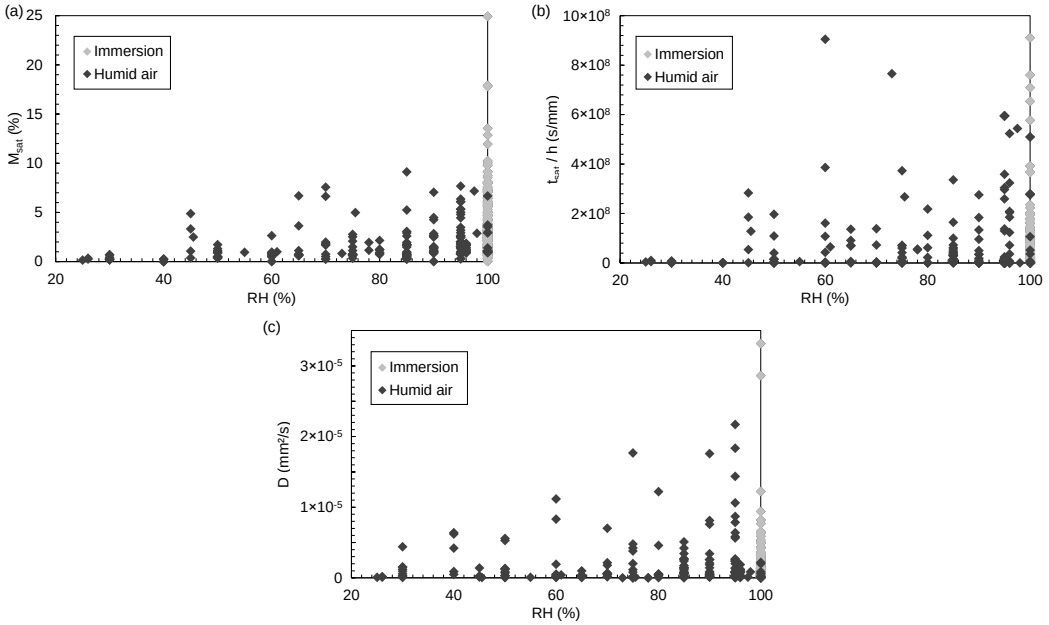

Figure 4. Evolution of (**a**) M_{sat}, (**b**) t_{sat}/h and (**c**) D as a function of relative humidity RH.

In immersion in a liquid, C_{sat} is related to the chemical potential of the water, i.e., it tends to decrease when the concentration of solutes increases [118]. The solvent concentration $[S]$ in an environment is in equilibrium with its partial pressure P_s in the atmosphere. There is a maximum concentration $[S]_{sat}$, which corresponds to the saturation pressure P_{sat} (Equation (14)).

$$\frac{P}{P_s} = \frac{[S]}{[S]_{sat}}. \tag{14}$$

If there is no extraction of soluble species, the polymer behaves in the same way in the liquid as in the saturated vapour. Indeed, equilibrium corresponds to the equality of the solvent chemical potentials in the polymer and in the environment. If the material is damaged, has pores or cracks, the solvent can also flow into it, as part of irreversible ageing. The presence of solutes in water, such as salt in seawater, causes the decrease of chemical potential, of saturation vapour pressure, and of solvent equilibrium concentration. Pure water causes greater moisture uptake than mineral water or seawater [20].

The diffusivity D also increases with the relative humidity in the environment. The calculation of this, according to the Fick model, is directly linked to M_{sat}, associated with the RH, and the thickness h (Equation (16)) [109,144]. For its part, the Carter *and* Kibler model links D to a number of free water molecules n and a number of bound water molecules N as a function of time t (Equation (16)) [45].

$$D = \frac{\pi}{16}\frac{h^2}{t}\left(\frac{M(t)}{M_{sat}}\right)^2 \tag{15}$$

$$D\frac{\delta^2 n}{\delta x^2} = \frac{\delta n}{\delta t} + \frac{\delta N}{\delta t}. \tag{16}$$

While M_{sat} and D increase with RH in the statistical study, t_{sat}/h evolution with RH is less evident. The high dispersion of this parameter does not allow us to conclude and is not suitable for a simple statistical dispersion study.

3.6.3. Temperature

The temperature T_{ageing} increase in the humid environment leads to accelerated ageing, as shown in the statistical study in Figure 5. The more important diffusion leads to an absorbed water mass stabilisation in a shorter time [33,39,54,55]. D, either Fick or Dual, is related to temperature by an Arrhenius law [37,145,146].

$$D = D_0\, exp(\frac{-E_a}{RT}). \tag{17}$$

T_{ageing} seems to increase D and to decrease t_{sat}/h. However, the strong dispersion of the data does not allow any conclusion.

In contrast, M_{sat} does not seem to be affected by the temperature. The non-relationship of saturation mass uptake with ageing temperature is under sorption isotherm laws such as Henry's. The saturation mass uptake does not depend on the temperature for the vast majority of studies, whether they are epoxy resins, epoxy-based composites, with varying reinforcements and architectures, Fick sorption kinetics or not. At 25 °C, epoxies have a solubility parameter δ close to 22 $MPa^{1/2}$, which is very far from the water solubility parameter, of 47.8 $MPa^{1/2}$ [117,147,148]. Water and epoxies are then hardly miscible. However, a higher temperature induces a decrease in the water solubility parameter while that of polymers remains reasonably constant or increases slightly. Substances that were not solvent can then become so . From an overall study point of view, and although there are exceptions, the variations in these two solubility parameter do not seem to be sufficient for the epoxies and the water to be miscible enough to induce a correlation between M_{sat} and T_{ageing}. For example, at 100 °C, the water solubility parameter is 44.4 $MPa^{1/2}$. That of the Epikote 828™/Epikure™ epoxy system increases from 21.9 at 25 °C to 22.5 $MPa^{1/2}$ at 100 °C [149].

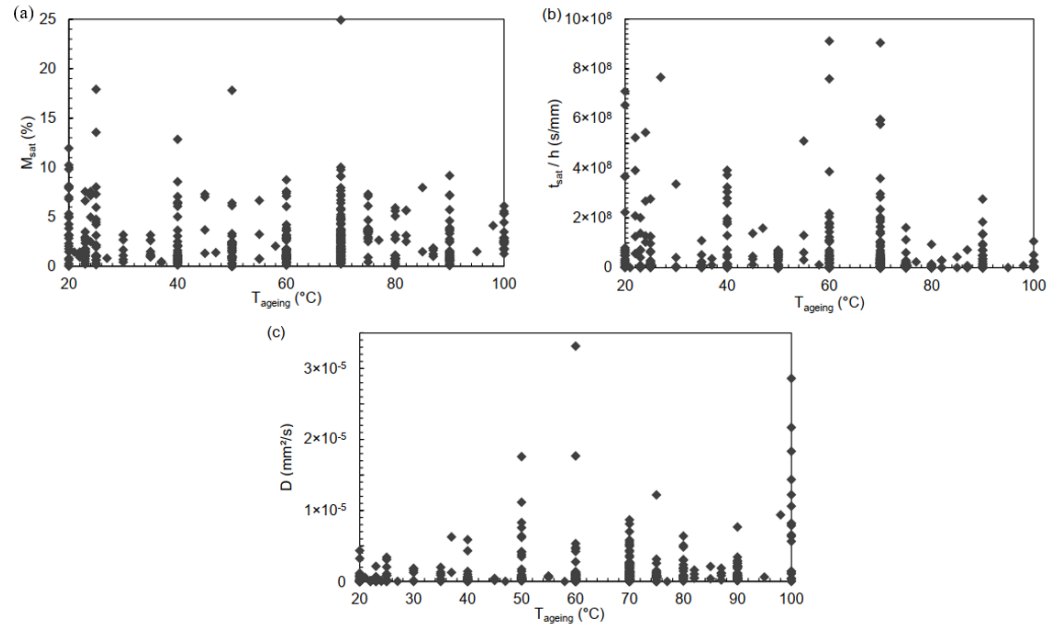

Figure 5. Evolution of (**a**) M_{sat}, (**b**) t_{sat}/h et (**c**) D as a function of the ageing temperature T_{ageing}.

However, as with the relative humidity, to observe the temperature correlations and be able to conclude, it is necessary to use another type of statistical analysis.

The wide dispersion of the data makes it difficult to conclude by simply observing the evolution of the variables in pairs. In addition, the data in the study show great heterogeneity due to a large number of prepolymers, hardeners and reinforcements, the diversity of processing methods, and the different conditioning parameters. All these parameters vary from one individual to another, which leads to other absorption behaviours, although irreversible behaviours have already been ruled out. A simple comparison of the variables in pairs is not sufficient to draw conclusions. To complete the statistical study, principal component analysis (PCA) is used in the rest of this paper.

4. Principal Component Analysis

4.1. Principal Component Analysis Introduction

The dataset used in this paper is associated with a large number of quantitative variables. Each of these variables can be related to a dimension. When the number of variables exceeds three, it is challenging to visualize a multidimensional space. Principal component analysis (PCA) can then be used. This is a multivariate statistical analysis method used when individuals are described by several quantitative variables, and it is used to determine the relationships between these different variables. PCA is based on the projection of a quantitative dataset belonging to a multidimensional space into several two-dimensional spaces. It simplifies the study by reducing the dimensions, i.e., the variable number, by highlighting principal components, which are linear combinations of the original variables. The n individuals are projected into a subspace of dimension q, which is the principal components space. To represent a data cloud S_i in a reduced space, we use a system of q linear combinations CP_q and p quantitative variables X^p. These linear combinations CP_q are the principal components [150,151].

PCA is particularly effective when the variables are highly correlated. In statistics and probability, studying the correlation between two variables is equivalent to studying the intensity of their links [114,116]. The correlations between variables and principal components can be read from a correlation circle of radius 1 where a vector of a given length represents each variable. The vector end coordinate corresponding to the variable on a principal component makes it possible to quantify its correlation. The closer the vector length is to 1, the better the variable is correlated in the principal component. It is also possible to observe correlations between variables if their vectors are long enough, so they are sufficiently well represented in the two-dimensional space. The correlation circle is interpreted as follows [152,153] :

- An acute angle (<90°) between the vectors of individual variables indicates a positive correlation between them;
- A 180° angle between the vectors of individual variables indicates a negative correlation between them;
- Variables whose vectors are orthogonal are not correlated with each other, and are therefore independent.

Therefore, principal component analysis enables, in addition to quantifying the correlation between a variable and a principal component, suggesting correlations between variables. The objective is to identify the dimensions or principal components along which the data variation is maximal. These data are represented in a system of X-Y coordinates. It is then possible to highlight relationships between variables that cannot be visualized in a space with more than two dimensions. Each individual in the study, characterized by these variables, is represented by a point. All these points form a data cloud described in a two-dimensional space. For the principal component analyses, the 448 individuals from the 90 publications are used. The set of variables is given in Table 8.

Table 8. List of variables used in the principal component analysis. The 8 qualitative variables are in italics and the 4 quantitative variables in Roman.

Material Parameters	Ageing Parameters	Diffusion Parameters
Prepolymer type	*Conditioning*	D
Hardener type	RH	M_{sat}
Reinforcement type	T_{ageing}	t_{sat}
h		M_{inter}
Process		t_{inter}
		β

4.2. Data Standardisation

A large dataset may contain heterogeneous individuals. This is particularly the case for some variables of our study, such as t_{sat} and D. It is then essential to center and reduce (i.e., to standardize) the dataset, which allows giving the same importance to the all the variables. The standardization is carried out so that the variables have a standard deviation equal to 1 and a mean value equal to 0 [116].

The PCA function of the package *FactoMineR* from *R* automatically normalises the data as explained above [116,154–156]. This function generates various indicators for each dimension or principal component: eigenvalues, variances, and cumulative variances. The eigenvalues can be used to determine the number of dimensions to keep for the study of the dataset. For this purpose, the data being centred-reduced, an eigenvalue of >1 is required. This means that the component concerned represents more variance than the original variable alone [157]. The eigenvalue quantifies the variance explained by each dimension. It is large for the first dimensions and small for the following ones (Table 9). Therefore, the first dimensions correspond to the directions that carry the maximum amount of variation contained in the dataset. PCA significantly reduces the number of principal components and compresses the variance into a smaller number of axes.

Table 9. Eigenvalues, variances and cumulative variances of the study dimensions.

Dimension	Eigenvalue	Variance	Cumulative Variance
Dim 1	2.18	27.19	27.19
Dim 2	1.55	19.39	46.58
Dim 3	1.13	14.09	60.68
Dim 4	0.88	11.10	71.78
Dim 5	0.86	10.73	82.52
Dim 6	0.79	9.84	92.37
Dim 7	0.58	7.19	99.56
Dim 8	0.03	0.43	100.00

Another method used to determine the number of the dimensions to choose from is to consider the graph or "scree plot" of the eigenvalues and stop at the level of the eigenvalue drop-off, beyond which they are relatively small (Figure 6) [150,158].

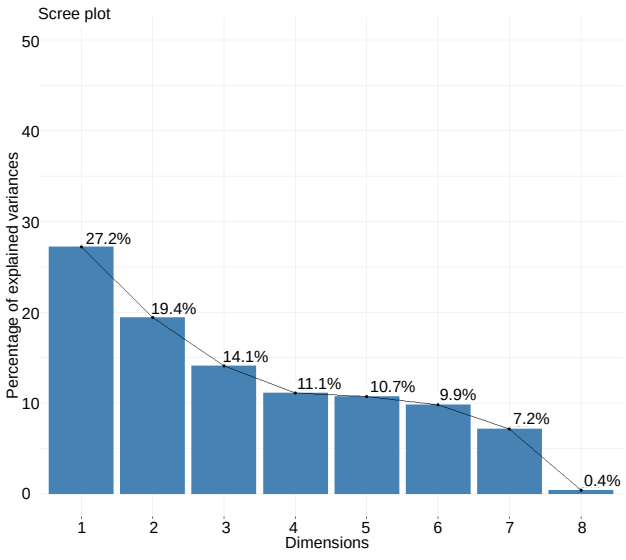

Figure 6. Eigenvalue scree plot.

If the whole dataset is considered, it could be possible to stop at the fourth principal component because its eigenvalue is less than 1. However, this only represents a cumulative variance of 60.7%. Looking at the eigenvalue graph, we do indeed see a drop-off at the

fourth principal component, but components with relatively large variance follow it. We can choose to stop at this 4th principal component or to stop at the 6th before the second drop-out, that is to say, a cumulative variance of 92.4%. The latter solution is chosen. In addition, by observing the representation quality of the variables, we note that some of them are adequately represented on the principal components 4 and 6. This is the case for D and RH. This large number of different variables explains this large number of components to be studied. There is no universal method to decide how many principal components to choose for PCA. It depends on the dataset, the variances of each component, but also on how well the variables are represented in the different components.

4.3. Results

4.3.1. Overview

By using the PCA method on the 448 individuals in this study, we obtain individual projection graphs and correlation circles that provide information on the relationship (or non-relationship) between the variables. For each principal component, an individual graph and a correlation circle are obtained. The first two principal components represent respectively 27.2% and 19.4% of the variance of the individuals, i.e., 46.6%. It is necessary to observe the first 6 components so that 92.4% of the variance of the individuals is represented, which makes it possible to have an overall vision of the latter. The number of variables to be studied is therefore reduced from 8 to 6 principal components. The variables which constitute them are determined by analysis of the "coordinate" of their vector on the component, which is the cosine of the angle formed between the vector and the principal component: a cosine close to 1 is desired to have an accurate representation of the component. The 6 Equations (18)–(23) below describe the principal components and their compositions, the coefficients being the coordinates of the variables in the principal component:

$$CP_1 = M_{sat} \times 0.96 + M_{inter} \times 0.95 + RH \times 0.55 + h \times 0.18 - T_{ageing} \times 0.08 + D \times 0.08 + t_{sat} \times 0.04 + t_{inter} \times 0.004 \quad (18)$$

$$CP_2 = t_{inter} \times 0.79 - T_{ageing} \times 0.67 + t_{sat} \times 0.59 - D \times 0.34 - M_{inter} \times 0.05 - M_{sat} \times 0.02 + h \times 0.01 + RH \times 0.01 \quad (19)$$

$$CP_3 = h \times 0.75 + D \times 0.53 + t_{sat} \times 0.35 + T_{ageing} \times 0.29 + t_{inter} \times 0.19 - M_{inter} \times 0.12 - M_{sat} \times 0.11 + RH \times 0.10 \quad (20)$$

$$CP_4 = - D \times 0.74 + T_{ageing} \times 0.40 + h \times 0.28 + t_{sat} \times 0.22 - t_{inter} \times 0.16 + RH \times 0.16 - M_{inter} \times 0.04 - M_{sat} \times 0.02 \quad (21)$$

$$CP_5 = t_{sat} \times 0.54 - h \times 0.53 + RH \times 0.40 + T_{ageing} \times 0.23 + D \times 0.20 - t_{inter} \times 0.13 - M_{inter} \times 0.10 - M_{sat} \times 0.05 \quad (22)$$

$$CP_6 = -RH \times 0.70 + t_{sat} \times 0.33 + T_{ageing} \times 0.27 + M_{sat} \times 0.23 + M_{inter} \times 0.21 - h \times 0.13 + D \times 0.03 + t_{inter} \times 0.02 \quad (23)$$

The first principal component is mainly composed of M_{sat}, M_{inter} and to a lower level RH: it is the material moisture absorption. The second main component is dominated by t_{inter}, t_{sat} and $-T_{ageing}$. The third component is represented by h and D: it may illustrate the diffusion through the thickness. The fourth principal component is $-D$. The fifth principal component is also represented by t_{sat} and h, but their coordinates are not very large, so their representation is not very good. Finally, the sixth principal component consists mainly of $-RH$, whose representation is not good either. For a specific variable, the sum of the squared cosines on all the principal components equals 1. As they add up according to the different principal components, the representation of the squared cosines of the coordinates of the variables makes it possible to quickly visualize which principal components they are associated with, their representation quality, and therefore which correlation circles to study subsequently. However, in the literature, no threshold value of squared cosines or coordinates is formally declared (Figure 7).

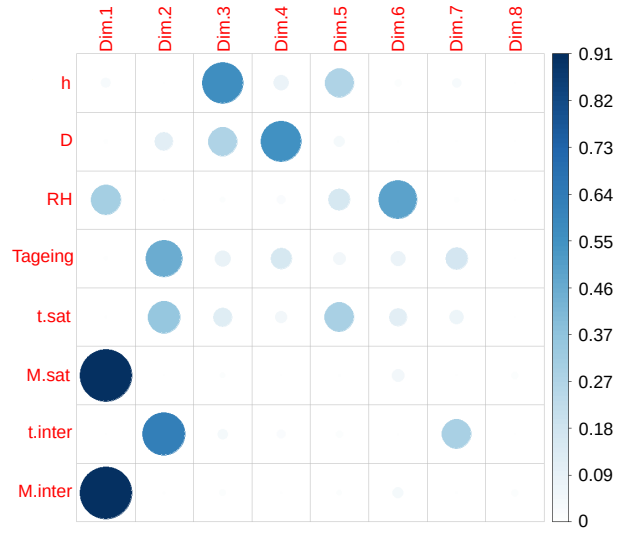

Figure 7. Representation quality of the study variables on the principal components of the overall PCA.

The correlation circles of the PCA, formed on the first 6 principal components, are then studied (Figure 8). The reduction by principal components allows us to limit the study to 6 and observe the variables by groups. It is already known that the variables of the following groups are correlated with each other because they are very well represented on their principal component:

- M_{sat} and M_{inter} are correlated with each other (CP_1);
- t_{sat} and t_{inter} are correlated with each other, and are anti-correlated with T_{ageing},which means they decrease when T_{ageing} increases (CP_2);
- h and D are correlated with each other (CP_3);

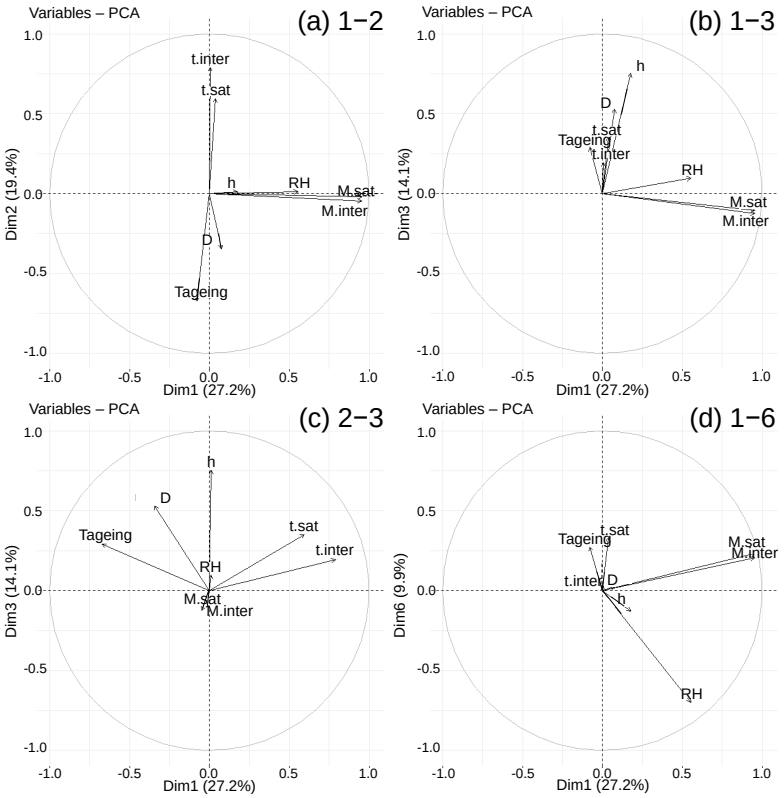

Figure 8. Correlation circles on planes (**a**) 1–2, (**b**) 1–3, (**c**) 2–3 and (**d**) 1–6 of the global PCA.

The vectors' placement representing the variables on the correlation circles is analyzed by taking into account their length. Figure 8 comprises the correlation circles of the 1–2, 1–3, 1–6 and 2–3 planes, which allow observation of all the analyses made in the following. The other circles, which do not provide more information, are not shown for the sake of clarity. RH, which was moderately well represented on principal component 1, is very well represented on component 6. The observation of the 1–6 plane confirms the correlation of M_{sat}, M_{inter} and RH. On the other hand, M_{sat} and M_{inter} are never correlated with the groups t_{sat}, t_{inter} and T_{ageing} or D and h, so their evolution is independent. A positive correlation is observed between D and T_{ageing} on the 2–3 plane, which is in agreement with the literature where Arrhenius laws are established between these two variables. Still on the 2–3 plane, h, t_{sat} and t_{inter} are correlated. The greater the h, the longer it takes to reach saturation time. Although t_{sat} and t_{inter} are anti-correlated with T_{ageing}, it is not possible to conclude on the correlation between the t_{sat} *and* t_{inter} group and D, their vectors not being of sufficient size. These observations are rather coherent with the conclusions made in the literature.

The points disposition on the individual graph is observed according to the diffusion behaviour type (Figure 9). Whether they follow a Fick law or a diffusion two-step derivative, most individuals are mixed in the graph centre. Nevertheless, there are only two-step specimens that extend along principal component 1, which represents M_{sat}, M_{inter} and RH. Furthermore, many samples in first part of the axis are Fick. Therefore, the strongest absorptions are associated with two-step materials, while the weakest are obtained with Fick materials, as we have observed with the box plots analysis. Points corresponding to the two types of behaviour studied stretch along component 2, which represents t_{sat}, t_{inter} and $-T_{ageing}$. Their intermediate and saturation times are therefore greater. Finally, the points that extend over component 3, corresponding to the thickness and the diffusivity, are associated with two-step diffusion materials. This material type, therefore, achieves the highest diffusivity.

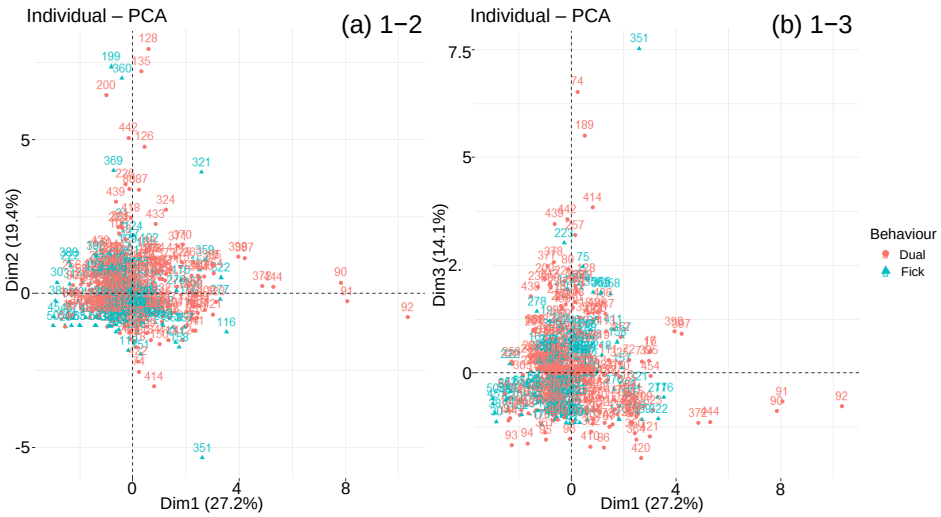

Figure 9. Graphs of individuals on planes (**a**) 1–2 and (**b**) 1–3 of the global PCA, according to diffusion behaviour.

The graphs of individuals along the principal components are now studied with respect to the qualitative variables presented previously. The objective is to highlight groupings according to one or more qualitative variables. However, the sorting according to the type of prepolymer or hardener does not clearly show any groups of individuals (Figures 10 and 11). All types of prepolymers and hardeners are mixed in the large cluster of graphs. Biobased epoxies, such as epoxidised soybean oil (ESO), blend into the cluster with typical M_{sat} and t_{sat} values [74]. The points that move away from the main cluster are not due to a difference in prepolymer or hardener.

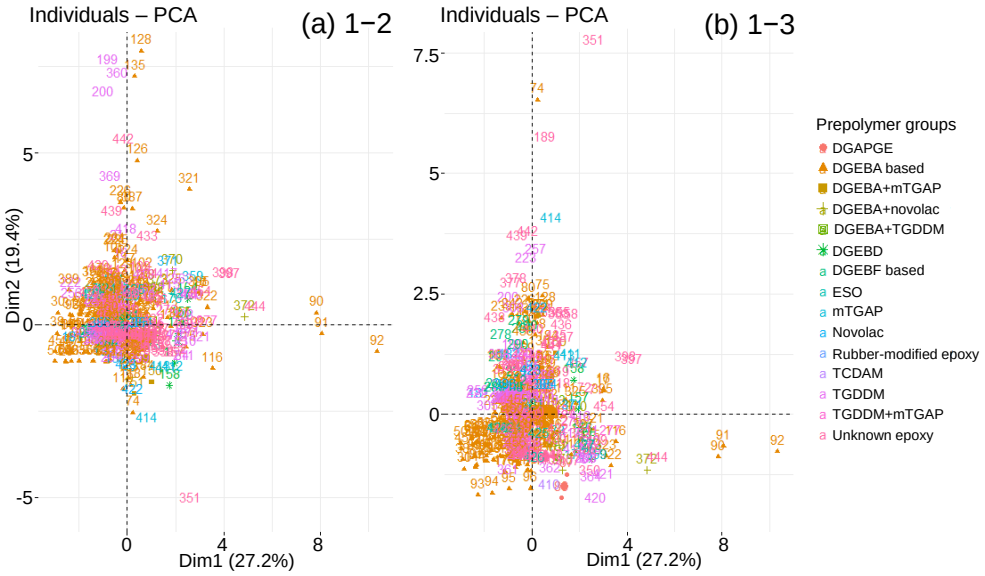

Figure 10. Graphs of individuals on planes (**a**) 1–2 and (**b**) 1–3 of the global PCA, according to prepolymer type.

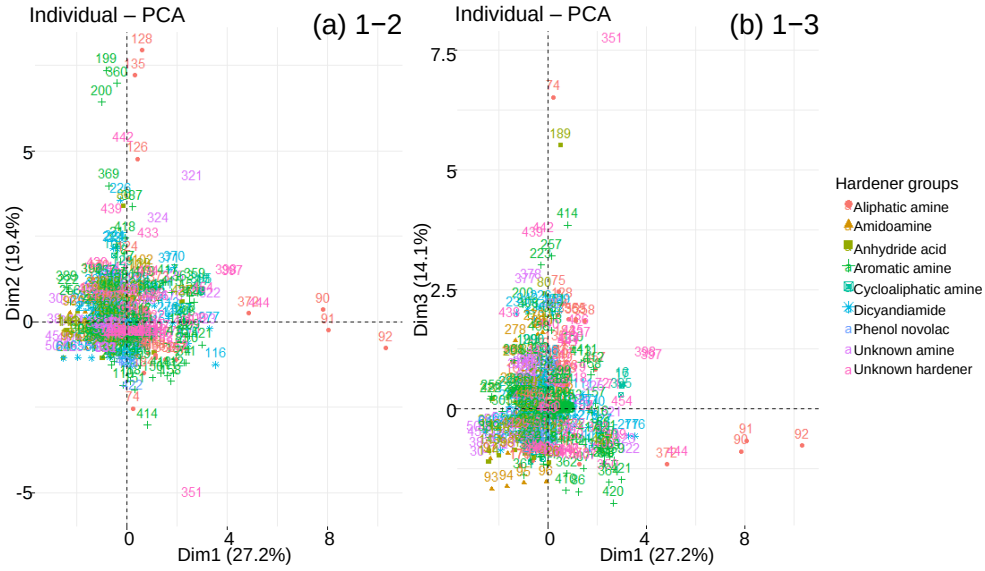

Figure 11. Graphs of individuals on planes (**a**) 1–2 and (**b**) 1–3 of the global PCA, according to hardener type.

Nevertheless, according to the reinforcement type, the graph makes it possible to distinguish several groupings on the 1–2 plane (Figure 12). In fact, towards the graph centre, the glass or carbon fibre composites are located. Then come the neat resins and finally the composites with flax, hemp, aramid and regenerated cellulose fibres. This group stretches along the principal component 1, which represents M_{sat}, M_{inter} and RH, which confirms the dispersion analysis as well as the literature: organic fibre composites absorb more water than inorganic fibre composites or even neat resins. Some points also stretch along component 2 which represents t_{sat}, t_{inter} and $-T_{ageing}$. Their intermediate and saturation times are therefore larger. These points represent carbon fibre composites and pure resins. There are no glass fibre composites.

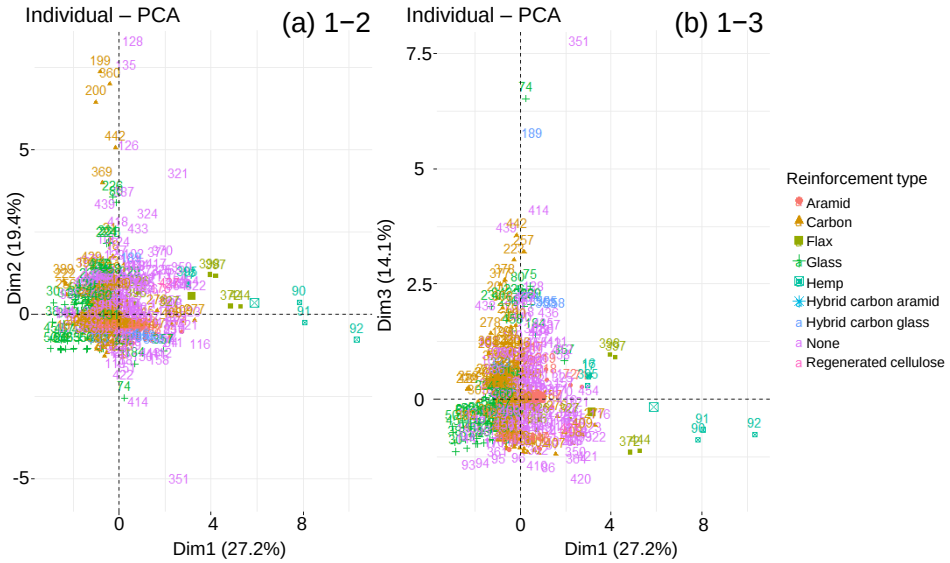

Figure 12. Graphs of individuals on planes (**a**) 1–2 and (**b**) 1–3 of the global PCA, according to reinforcement type.

By making the same observations with the type of conditioning, a cluster representing humid air and a cluster representing water are noticeable, whether distilled, seawater or deionised water (Figure 13). The humid air cluster is located in the left part of the first principal component. The individuals in this cluster, due to their smaller RH, show below-average M_{sat} and M_{inter} values. The water cluster extends along with component 1. High water mass uptakes distinguish several individuals immersed in distilled water. The two clusters are stretched along with components 2 and 3, which involve individuals with very long intermediate and saturation times for low temperatures. However, the individuals immersed in water with longer times are still more important than those under air.

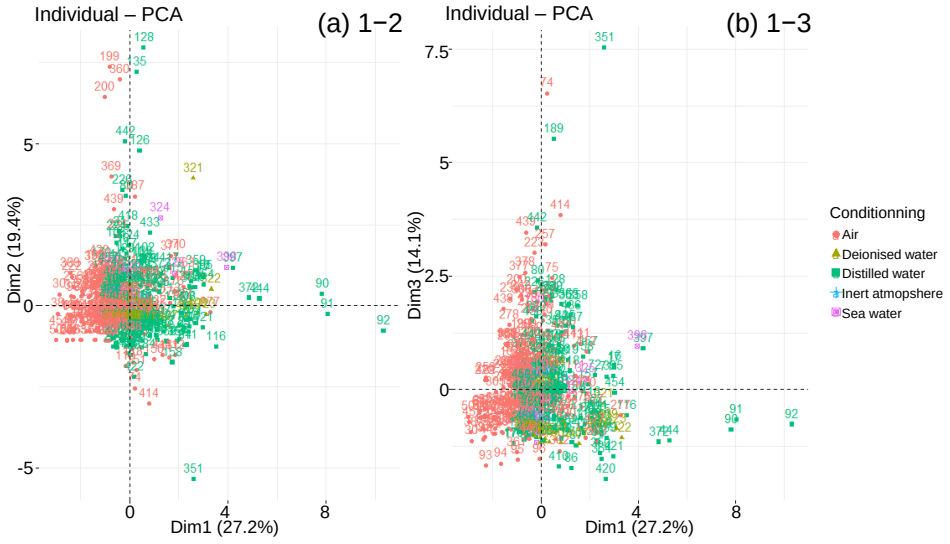

Figure 13. Graphs of individuals on planes (**a**) 1–2 and (**b**) 1–3 of the global PCA, according to conditioning environment.

About the manufacturing process, no data clustering is distinguished, except for the infused individuals that extend along with the first principal component (Figure 14).

The current dataset mixes neat resins and composite materials, but also materials with different absorption behaviour. The graph of individuals shows us clusters according to the diffusion behaviour and the presence or not of reinforcement as well as its nature.

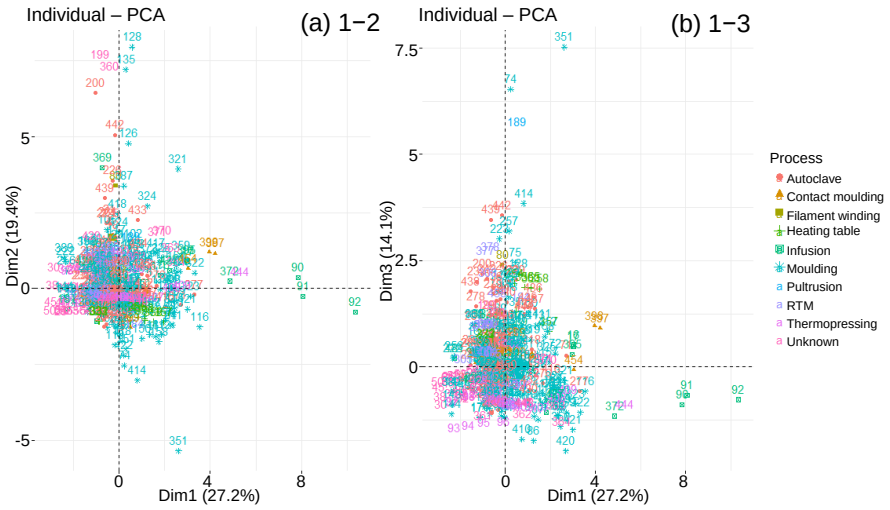

Figure 14. Graphs of individuals on planes (**a**) 1–2 and (**b**) 1–3 of the global PCA, according to manufacturing process.

For the continuation of the PCA study, the individuals are separated into four classified PCA according to their nature-neat resins or composites-and according to their moisture diffusion behaviour—Fick or Dual (Table 10). The objective is to study more precisely the correlations between variables, to compare the different behaviours, to further group the variables into principal components and to observe if new groupings of individuals are made. This separation of individuals also allows the introduction of variables not studied up to this point of the document. For composite materials, these variables are the fibre volume fraction and the fibre architecture. For Dual behaviour, they are M_{inter}, t_{inter}, β, γ and K, which are parameters linked to the Dual–Fick, and Carter *and* Kibler models, but have no meaning for the Fick model. As a reminder, M_{inter} and t_{inter} are respectively the values of the mass of water absorbed and the time at the intermediate stage. β is the probability that bound water molecules will be liberated, and γ is the probability that free water molecules will be bound. β and γ, therefore, illustrate the changes in the state of the water molecules that modify the diffusion behaviour of the materials. Finally, K is a parameter related to the swelling of the polymer (Table 11).

Table 10. Separation of the study individuals into four classified PCA groups.

	All	Resins, Fick	Composites, Fick	Resins, Dual	Composites, Dual
Individual number	448	56	98	147	147
Initial variables number	8	6	7	11	12
Individual variance of each initial variable	12.5%	16.7%	14.3%	9.1%	8.3%
Min. number of PC for an overview	6 (92.4%)	4 (85%)	4 (79.6%)	5 (76.3%)	6 (79.4%)

Table 11. List of variables used in the four classified principal component analysis. The 12 qualitative variables are in italics and the 7 quantitative variables in roman.

Material Parameters	Ageing Parameters	Diffusion Parameters
Prepolymer type	Conditioning	D
Hardener type	RH	M_{sat}
Reinforcement type	T_{ageing}	t_{sat}
Architecture		M_{inter}
Fibre orientation		t_{inter}
v_f		β
h		γ
Process		K

4.3.2. Classified PCA

On correlation circles, it is possible to distinguish four main groups of variables present in all the four classified PCA (Figure 15). M_{sat}, M_{inter} and RH represent moisture absorption. The T_{ageing}, D and h relate to the water diffusion speed. β, γ, K and D are associated with the water molecule diffusion and their placement. t_{sat}, t_{inter} and v_f are linked to the saturation time. This allows reducing the variable number. For example, the variables β, γ and K of the Carter *and* Kibler model are related to D. We also see the relationships between the different variables, confirming the experimental studies and models reported in the literature.

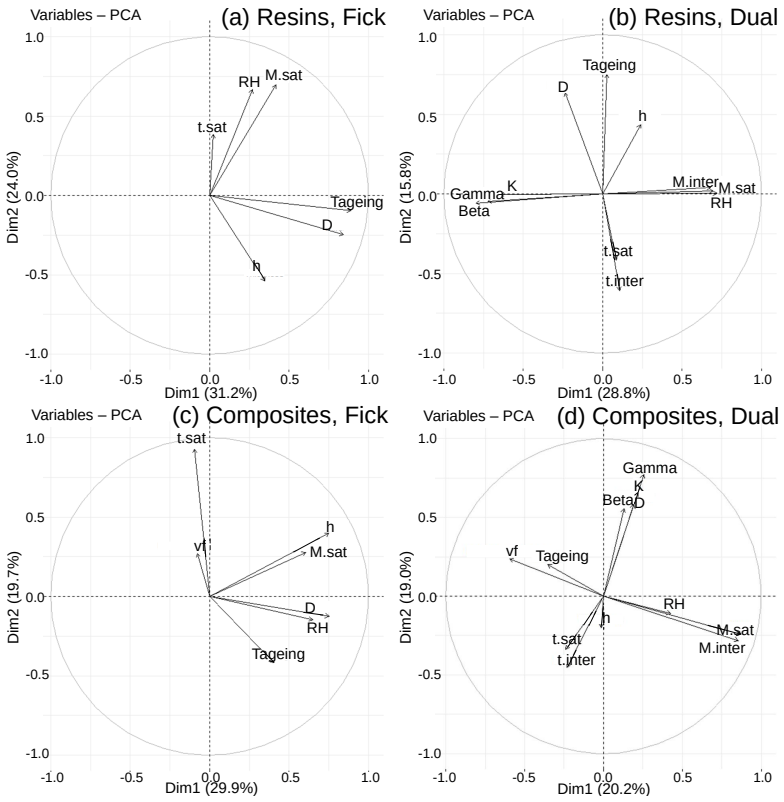

Figure 15. Correlation circles on the 1–2 planes of classified PCA: (**a**) Fick resins, (**b**) Dual resins, (**c**) Fick composites and (**d**) Dual composites. Further planes are given as Supplementary Materials: Fick resins in Figure S21, Fick composites in Figure S22, Dual resins in Figure S23 and Dual composites in Figure S24.

The classified PCA also showed differences. Depending on the material type (neat resin or composite) and the behaviour (Fick or Dual), further conclusions of correlation, anti-correlation or non-correlation can be made. In contrast, limited variations are observed depending on the nature of the epoxy prepolymer or hardener. In the case of neat resins and Fick composites, D depends on T_{ageing}, M_{sat} on RH and t_{sat} on T_{ageing}. In case of the fibre presence, t_{sat} is also influenced by v_f. All these parameters also depend on h, as Fick diffusion occurs in the material thickness, without chemical interaction.

For Dual diffusion materials, some correlations are modified in comparison with Fick diffusion materials. For neat resins, M_{sat} is dependent on h as for Fick materials, while for composites, it becomes independent. Moreover, t_{sat}, which is independent of D for Fick resins, becomes anti-correlated for Dual behaviour. M_{sat} changes from being correlated with D for Fick diffusion behaviour to being uncorrelated for Dual diffusion behaviour.

In neat resins, β, γ and K are correlated with D, anti-correlated with M_{sat} and uncorrelated with t_{sat}. For composites, β, γ and K are always correlated with D and T_{ageing}. T_{ageing} accelerates diffusion. It indirectly accelerates the propagation and the bonding and unbonding processes of water molecules. However, β, γ and K become uncorrelated with

M_{sat} and anti-correlated with t_{sat}. From the graphs of the individuals, these three variables are more important when the material is exposed to humid air rather than immersed, which may suggest that moisture diffusion is more complex in the air than in water. It should also be noted that v_f become anti-correlated with M_{sat} and correlated with t_{sat}, whereas, for the Fick cases, these two last parameters were not related to the mass uptake. The presence or absence of fibres has a strong impact on diffusion behaviour. Indeed, the increase of v_f decreases the mass water uptake. When there are too many fibres, they act as a barrier for the free water molecules, which diffuse in smaller numbers and more slowly. Different interactions may take place between the fibres and the water molecules, as differences are observed in the graphs of individuals representing the type of reinforcement used.

5. Discussion

With box plots, natural organic fibres appear to be the most sensitive to water, followed by aramid fibres which are synthetic organic fibres. In the study, composites based on organic fibres have a Dual behaviour. The presence of hydrophilic functional groups on their macromolecular skeleton amplifies the diffusion and moisture absorption, which can be higher than that of neat resins. Inorganic fibres such as glass and carbon have lower absorption percentages due to their impermeability. However, they still impact diffusion as they create differential swellings at the fibre/matrix interface leading to concentration gradients and possible degradations.

Another major difference highlighted by the correlation circles is the anti-correlation between T_{ageing} and M_{sat} in the case of Dual composites. M_{sat} is then influenced by T_{ageing} whereas it should not be in reversible diffusion models. Moreover, β, γ and K are parameters associated with the binding of water molecules to macromolecules. They change from correlated to M_{sat} for Dual Resins to uncorrelated for Dual Composites.

It is known that when the behaviour derives from the Fick model, the diffusion is not only due to the propagation of water molecules in the free volumes. Bonding interactions can take place between these water molecules and the material. These changes can lead to chemical degradation such as hydrolysis, chain breaks or oxidation. Hygroscopic swelling, cracking, osmotic damage and loss of admixtures or particles may occur [6,8,103,159–163]. In some cases, which were not studied in this paper, the gravimetry curves enable to observe these degradations, which are expressed by significant mass losses [7,22,105,112]. In other cases, weak irreversible alterations can take place in the material during hygrothermal ageing while having a two-stage diffusion. This is the case for many under-crosslinked industrial epoxy systems, which contain unreacted oxirane groups or polar compounds such as amines. These groups, which are very hydrophilic, become preferential sites for the formation of hydrogen bonds, for the initiation of hydrolysis and for the creation of concentration gradients [10,72]. As well, the sizing used on the fibres, the additives added to the matrix and the organic fibres can be hydrophilic, degrade with water and create osmotic degradation [29,133,160,164]. These irreversible modifications, which are hardly perceptible on the absorption gravimetry curve, can be observed by desorption. The mass variation $M(t)$ does not return to its initial value. Mass losses therefore occur during the absorption phase while the mass gain curve continues to increase slowly. Studying the desorption kinetics is then important to verify the presence of hidden mass losses or to highlight a chemical evolution [12,72,165–168]. As with the Fick equation, the Carter *and* Kibler and Dual–Fick equations model purely physical diffusion kinetics. When chemical degradation takes place, these models may no longer be representative of the material absorption behaviour. If irreversible phenomena enter the diffusion kinetics, it is possible that this will change the correlations between the different parameters. Because of T_{ageing} and M_{sat} anti-correlation, it is then conceivable that in a non-negligible number of cases, the behaviour of the individuals in the study is not purely related to physical diffusion. Degradations, although slight, may be present, making the chosen model inaccurate. Although the gravity curves fit well, the associated parameters may no longer represent the mechanisms for which they were chosen, such as *beta*, *gamma* and *K*. The consequences of an inappropriate model choice are the premature termination of gravimetric monitoring

of materials, the non-detection of degradation phenomena that may appear at longer absorption times, inaccurate estimates of M_{sat} whose true value is masked by mass losses, and the performance of material characterisation at inappropriate M_{sat} [169,170].

6. Conclusions

In this paper, statistical tools were used to study how the parameters related to hygrothermal ageing influence each other. For this purpose, data were extracted presenting scientific publications from experimental tests carried out on neat epoxy resins and epoxy-based composites. The analysis started with a scattering study of the three most characteristic variables of hygrothermal ageing: saturation mass uptake M_{sat}, saturation time t_{sat} and diffusivity D, using box plots and scatter plots. The box plots enable us to differentiate these three parameters as a function of some qualitative parameters, such as pre-polymers type, reinforcement type, or process. The results obtained are in accordance with the observations made in the literature.

On the other hand, parameters such as hardener type or architecture reinforcement are more difficult to differentiate, as they are strongly linked to other parameters. For the quantitative parameters v_f, RH and T_{ageing}, the analyses are also more complex due to the high dispersion of the data coming from very diverse individuals.

These results led to combining the dispersion analysis with another type of statistical analysis: principal component analysis (PCA). This analysis, which centres and reduces the variables when they are highly dispersed, simplifies the study despite the variation of many parameters and allows the deduction of correlations between variables. PCA was then performed on different groups of data, classified according to the material nature (neat resin or composite) and the diffusion behaviour (Fick diffusion, or Dual diffusion), to observe if any differences are noticeable. Some connections between variables, identified in the correlations circles and graphs of individuals of the PCA, have been demonstrated many times in the literature. The study becomes more complex with the Dual diffusion behaviour composites. Some correlations between parameters change. In particular, D and T_{ageing}, correlated in the global PCA, become independents in the PCA of Dual composites. These changes do not correspond to the reversible diffusion models. It seems that, despite a two-step diffusion curve, without apparent mass losses in gravimetry, the Carter *and* Kibler or Dual–Fick models and their parameter do not seem to fit all individuals.

However, the study carried out in this paper has some limitations, due to the quality of representation of some variables, especially in the dual sorption composites PCA. Global PCA does not result in a significant reduction in the number of principal components (-2), although the classified PCA results in better reductions (from -2 to -6). PCA does not allow any remarkable differentiation according to the nature of the epoxies and their hardeners, as this type of polymer is hydrophilic and hygrothermal ageing depends on many parameters. In these two cases, the box plots allow a better visualisation of the data.

Other variables can be added to extend the study, such as mechanical properties, but this requires that these data have been reported in the literature, which is not always the case.

Supplementary Materials: The following supporting information can be downloaded at: https://www.mdpi.com/article/10.3390/polym14142832/s1, Figure S1: List of epoxy prepolymers, Figure S2: List of hardeners, Figures S3–S20: Box plots of D, t_{sat}/h and M_{sat} as a function of the study quantitative variables; Figure S21: Fick resins' PCA; Figure S22: Fick composites' PCA; Figure S23: Dual resins' PCA; Figure S24: Dual composites' PCA.

Author Contributions: Conceptualization, C.G., B.H.-R. and V.N.; methodology, C.G., F.T., B.H.-R. and V.N.; software, C.G. and F.T.; validation, C.G., F.T. and V.N.; formal analysis, C.G., F.T. and V.N.; investigation, C.G.; resources, B.H.-R., T.T. and V.N.; data curation, C.G.; writing—original draft preparation, C.G., F.T. and V.N.; writing—review and editing, C.G., F.T. and V.N.; supervision, V.N.; project administration, T.T. and V.N.; funding acquisition, T.T. and V.N. All authors have read and agreed to the published version of the manuscript.

Funding: This research was funded by Association Nationale de la Recherche et de la Technologie (ANRT) and SAFRAN Aircraft Engines through a CIFRE PhD fellowship: grant number n°2018/0355. The APC was funded by ANRT.

Institutional Review Board Statement: Not applicable.

Informed Consent Statement: Not applicable.

Data Availability Statement: The data presented in this study are available on request from the corresponding author.

Conflicts of Interest: The authors declare no conflict of interest.

References

1. Henry, L.; Kris, N. *Handbook of Epoxy Resins*; McGraw-Hill: New York, NY, USA, 1967.
2. Peters, S.T. (Ed.) *Handbook of Composites*, 2nd ed.; Springer Science and Business Media: Dordrecht, The Netherlands, 1998.
3. Jones, C.; Dickson, R.; Adam, T.; Reiter, H.; Harris, B. The environmental fatigue behaviour of reinforced plastics. *Proc. R. Soc. Lond. A. Math. Phys. Sci.* **1984**, *396*, 315–338.
4. Cavasin, M.; Sangermano, M.; Thomson, B.; Giannis, S. Exposure of Glass Fiber Reinforced Polymer Composites in Seawater and the Effect on Their Physical Performance. *Materials* **2019**, *12*, 807. [CrossRef]
5. Tsai, Y.; Bosze, E.; Barjasteh, E.; Nutt, S. Influence of hygrothermal environment on thermal and mechanical properties of carbon fiber/fiberglass hybrid composites. *Compos. Sci. Technol.* **2009**, *69*, 432–437. [CrossRef]
6. Lee, M.C.; Peppas, N.A. Water transport in graphite/epoxy composites. *J. Appl. Polym. Sci.* **1993**, *47*, 1349–1359. [CrossRef]
7. Zhou, J.; Lucas, J. The effects of a water environment on anomalous absorption behavior in graphite/epoxy composites. *Compos. Sci. Technol.* **1995**, *53*, 57–64. [CrossRef]
8. Weitsman, Y. Anomalous fluid sorption in polymeric composites and its relation to fluid-induced damage. *Compos. Part A Appl. Sci. Manuf.* **2006**, *37*, 617–623. [CrossRef]
9. Tsotsis, T. Considerations of failure mechanisms in polymer matrix composites in the design of aerospace structures. In *Failure Mechanisms in Polymer Matrix Composites*; Elsevier: Amsterdam, The Netherlands, 2012; pp. 227–278. [CrossRef]
10. Tcharkhtchi, A.; Bronnec, P.; Verdu, J. Water absorption characteristics of diglycidylether of butane diol–3,5-diethyl-2,4-diaminotoluene networks. *Polymer* **2000**, *41*, 5777–5785. [CrossRef]
11. Colin, X.; Verdu, J. Humid Ageing of Organic Matrix Composites. In *Durability of Composites in a Marine Environment. Solid Mechanics and Its Applications*; Davies, P., Rajapakse, Y.D.S., Eds.; Springer: Dordrecht, The Netherlands, 2014; pp. 47–114.
12. Deroiné, M.; Le Duigou, A.; Corre, Y.M.; Le Gac, P.Y.; Davies, P.; César, G.; Bruzaud, S. Accelerated ageing of polylactide in aqueous environments: Comparative study between distilled water and seawater. *Polym. Degrad. Stabil.* **2014**, *108*, 319–329. [CrossRef]
13. Boukhoulda, B.; Adda-Bedia, E.; Madani, K. The effect of fiber orientation angle in composite materials on moisture absorption and material degradation after hygrothermal ageing. *Compos. Struct.* **2006**, *74*, 406–418. [CrossRef]
14. Selzer, R.; Friedrich, K. Mechanical properties and failure behaviour of carbon fibre-reinforced polymer composites under the influence of moisture. *Compos. Part A Appl. Sci. Manuf.* **1997**, *28*, 595–604. [CrossRef]
15. De'Nève, B.; Shanahan, M. Water absorption by an epoxy resin and its effect on the mechanical properties and infra-red spectra. *Polymer* **1993**, *34*, 5099–5105. [CrossRef]
16. Ramirez, F.A.; Carlsson, L.A.; Acha, B.A. Evaluation of water degradation of vinylester and epoxy matrix composites by single fiber and composite tests. *J. Mater. Sci.* **2008**, *43*, 5230–5242. [CrossRef]
17. Halpin, J.C. *Effects of Environmental Factors on Composite Materials*; Technical report AFML-TR-67-423; Air Force Materials Laboratory, Wright-Patterson Air Force Base: Dayton, OH, USA, 1969; p. 45433.
18. Chen, C. Contribution à la Prise en Compte des Effets de l'Environnement sur la Tolérance aux Dommages d'Impact de Stratifiés Composites. Ph.D. Thesis, Institut Supérieur d'Aéronautique et de l'Espace, Paris, France, 2015.
19. Popineau, S.; Rondeau-Mouro, C.; Sulpice-Gaillet, C.; Shanahan, M.E. Free/bound water absorption in an epoxy adhesive. *Polymer* **2005**, *46*, 10733–10740. [CrossRef]
20. Fayolle, B.; Verdu, J. *Vieillissement Physique des Matériaux Polymères*; Techniques de l'Ingénieur: Paris, France, 2005; p. 22.
21. Grangeat, R. Durabilité des Assemblages Collés en Environnement Humide—Instrumentation par Capteurs à Fibre Optique. Ph.D. Thesis, Université de Nantes, Institut de Recherche en Génie Civil et Mécanique (GeM), Nantes, France, 2019.
22. Bonniau, P.; Bunsell, A.R. A comparative study of water absorption theories applied to glass epoxy composites. *J. Compos. Mater.* **1981**, *15*, 272–293. [CrossRef]
23. Morel, E.; Bellenger, V.; Verdu, J. Structure-water absorption relationships for amine-cured epoxy resins. *Polymer* **1985**, *26*, 1719–1724. [CrossRef]
24. Wong, K.J. Moisture Absorption Characteristics and Effects on Mechanical Behaviour of Carbon/Epoxy Composite: Application to Bonded Patch Repairs of Composite Structures. Ph.D. Thesis, Université de Bourgogne, Laboratoire DRIVE ISAT, Nevers, France, 2014.

25. Soles, C.L.; Yee, A.F. A Discussion of the Molecular Mechanisms of Moisture Transport in Epoxy Resins. *J. Polym. Sci. Part B Polym. Phys.* **2000**, *38*, 792–802. [CrossRef]
26. Abdelkader, A.F.; White, J.R. Water absorption in epoxy resins: The effects of the crosslinking agent and curing temperature. *J. Appl. Polym. Sci.* **2005**, *98*, 2544–2549. [CrossRef]
27. Sala, G. Composite degradation due to fluid absorption. *Compos. Part B Eng.* **2000**, *31*, 357–373. [CrossRef]
28. Doğan, A.; Arman, Y. The Effect of Hygrothermal Aging on the Glass and Carbon Reinforced Epoxy Composites for different Stacking Sequences. *Mechanics* **2018**, *24*, 19–25. [CrossRef]
29. Ray, B.C. Temperature effect during humid ageing on interfaces of glass and carbon fibers reinforced epoxy composites. *J. Colloid Interface Sci.* **2006**, *298*, 111–117. [CrossRef]
30. Augl, J.M.; Berger, A.E. *The Effect of Moisture on Carbon Fiber Reinforced Epoxy Composites. I. Diffusion*; Technical Report 76-7; White Oak Laboratory, Naval Surface Weapons Center: Silver Spring, MA, USA, 1976.
31. Clark, G.; Saunders, D.; van Blaricum, T.; Richmond, M. Moisture absorption in graphite/epoxy laminates. *Compos. Sci. Technol.* **1990**, *39*, 355–375. [CrossRef]
32. Gupta, V.B.; Drzal, L.T.; Rich, M.J. The physical basis of moisture transport in a cured epoxy resin system. *J. Appl. Polym. Sci.* **1985**, *30*, 4467–4493. [CrossRef]
33. Arnold, C.; Korkees, F.; Alston, S. The long-term water absorption and desorption behaviour of carbon-fibre/epoxy composites. In Proceedings of the ECCM15 Proceedings, ESCM: 15th European Conference on Composite Materials, Venice, Italy, 24–28 June 2012; Volume 15.
34. Simar, A. Impact du Vieillissement Humide sur le Comportement d'un Composite à Matrice Organique Tissé Fabriqué par Injection RTM: Mise en Evidence d'un Couplage entre Absorption d'Eau et Thermo-Oxydation de la Matrice. Ph.D. Thesis, École Nationale Supérieure de Mécanique et d'Aérotechnique, Institut Prime, Poitiers, France, 2014.
35. Kondo, K.; Taki, T. Moisture Diffusivity of Unidirectional Composites. *J. Compos. Mater.* **1982**, *16*, 82–93. [CrossRef]
36. Grangeat, R.; Girard, M.; Lupi, C.; Leduc, D.; Jacquemin, F. Measurement of the local water content of an epoxy adhesive by fiber optic sensor based on Fresnel reflection. *Mech. Syst. Sign. Process.* **2020**, *141*, 106439. [CrossRef]
37. Shen, C.H.; Springer, G.S. Moisture absorption and desorption of composite materials. *J. Compos. Mater.* **1976**, *10*, 2–20. [CrossRef]
38. Perreux, D.; Suri, C. A study of the coupling between the phenomena of water absorption and damage in glass/epoxy composite pipes. *Compos. Sci. Technol.* **1997**, *57*, 1403–1413. [CrossRef]
39. Pierron, F.; Poirette, Y.; Vautrin, A. A novel procedure for identification of 3D moisture diffusion parameters on thick composites: theory, validation and experimental results. *J. Compos. Mater.* **2002**, *36*, 2219–2243. [CrossRef]
40. Zainuddin, S.; Hosur, M.; Zhou, Y.; Kumar, A.; Jeelani, S. Durability studies of montmorillonite clay filled epoxy composites under different environmental conditions. *Mater. Sci. Eng. A* **2009**, *507*, 117–123. [CrossRef]
41. Frank, K.; Childers, C.; Dutta, D.; Gidley, D.; Jackson, M.; Ward, S.; Maskell, R.; Wiggins, J. Fluid uptake behavior of multifunctional epoxy blends. *Polymer* **2013**, *54*, 403–410. [CrossRef]
42. Sugita, Y.; Winkelmann, C.; La Saponara, V. Environmental and chemical degradation of carbon/epoxy lap joints for aerospace applications, and effects on their mechanical performance. *Compos. Sci. Technol.* **2010**, *70*, 829–839. [CrossRef]
43. Gaussens, C. Solutions Adhésives et Durabilité d'une Liaison Structurale d'un Capteur Céramique sur un Roulement Acier. Ph.D. Thesis, Institut National Polytechnique de Toulouse, Laboratoire Génie de Production (INP-ENIT), Tarbes, France, 2010.
44. Billy, F. Vieillissement et Propriétés Résiduelles de Matériaux Issus du Démantèlement d'Avions en Fin de Vie. Ph.D. Thesis, École nationale Supérieure de Mécanique et d'Aérotechnique, Institut Prime, Poitiers, France, 2013.
45. Carter, H.G.; Kibler, K.G. Langmuir-Type Model for Anomalous Moisture Diffusion In Composite Resins. *J. Compos. Mater.* **1978**, *12*, 118–131. [CrossRef]
46. Selzer, R.; Friedrich, K. Influence of water up-take on interlaminar fracture properties of carbon fibre-reinforced polymer composites. *J. Mater. Sci.* **1995**, *30*, 334–338. [CrossRef]
47. Zafar, A.; Bertocco, F.; Schjødt-Thomsen, J.; Rauhe, J. Investigation of the long term effects of moisture on carbon fibre and epoxy matrix composites. *Compos. Sci.Technol.* **2012**, *72*, 656–666. [CrossRef]
48. Choi, H.S.; Ahn, K.J. Hygroscopic aspects of epoxy/carbon fiber composite laminates in aircraft environments. *Compos. Part A Appl. Sci. Manuf.* **2001**, *32*, 709–720. [CrossRef]
49. Nguyen, T.H. Vieillissement Artificiel et Vieillissement Naturel en Ambiance Tropicale de Composites Modèles Epoxy/Verre: Approche Nanoscopique de l'Etude des Interphases. Ph.D. Thesis, Université du Sud-Toulon-Var, Laboratoire Matériaux Polymères-Interfaces-Environnement Marin, La Garde, France, 2013.
50. Zhou, J.; Lucas, J.P. Hygrothermal effects of epoxy resin. Part I: The nature of water in epoxy. *Polymer* **1999**, *40*, 5505–5512. [CrossRef]
51. Barton, S.J.; Pritchard, G. The moisture absorption characteristics of crosslinked vinyl terminated polyethers compared with epoxies. *Polym. Adv. Technol.* **1994**, *5*, 245–252. [CrossRef]
52. Weitsman, Y.J.; Guo, Y.J. A correlation between fluid-induced damage and anomalous fluid sorption in polymeric composites. *Compos. Sci. Technol.* **2002**, *62*, 889–908. [CrossRef]
53. Pérez-Pacheco, E.; Cauich-Cupul, J.I.; Valadez-González, A.; Herrera-Franco, P.J. Effect of moisture absorption on the mechanical behavior of carbon fiber/epoxy matrix composites. *J. Mater. Sci.* **2013**, *48*, 1873–1882. [CrossRef]
54. Dao, B.; Hodgkin, J.H.; Krstina, J.; Mardel, J.; Tian, W. Accelerated aging versus realistic ageing in aerospace composite materials. IV. Hot/wet ageing effects in a low temperature cure epoxycomposite. *J. Appl. Polym. Sci.* **2007**, *106*, 4264–4276. [CrossRef]

55. Dao, B.; Hodgkin, J.; Krstina, J.; Mardel, J.; Tian, W. Accelerated aging versus realistic aging in aerospace composite materials. V. The effects of hot/wet aging in a structural epoxy composite. *J. Appl. Polym. Sci.* **2010**, *115*, 901–910. [CrossRef]
56. Verghese, K.; Haramis, J.; Patel, S.; Senne, J.; Case, S.; Lesko, J. Enviro-mechanical durability of polymer composites. In Proceedings of the Long Term Durability of Structural Materials Workshop, Berkeley, CA, USA, 26–27 October 2001; pp. 121–132. [CrossRef]
57. Delozanne, J.; Desgardin, N.; Coulaud, M.; Cuvillier, N.; Richaud, E. Failure of epoxies bonded assemblies: Comparison of thermal and humid ageing. *J. Adhes.* **2018**, 1–24. [CrossRef]
58. Guermazi, N.; Haddar, N.; Elleuch, K.; Ayedi, H. Investigations on the fabrication and the characterization of glass/epoxy, carbon/epoxy and hybrid composites used in the reinforcement and the repair of aeronautic structures. *Mater. Des.* **2014**, *56*, 714–724. [CrossRef]
59. Dexter, H.B.; Baker, D.J. Flight service environmental effects on composite materials and structures. *Adv. Perform. Mater.* **1994**, *1*, 51–85. [CrossRef]
60. Vodicka, R.; Nelson, B.; van der Berg, J.; Chester, R. *Long-Term Environmental Durability of F/A-18 Composite Material*; Technical Report DSTO-TR-0826; DSTO Aeronautical and Maritime Research Laboratory: Melbourne, Australia, 1999.
61. McKague, E.; Halkias, J.; Reynolds, J. Moisture in composites: The effect of supersonic service on diffusion. *J. Compos. Mater.* **1975**, *9*, 2–9. [CrossRef]
62. Aktas, L.; Hamidi, Y.; Altan, M.C. Effect of Moisture Absorption on Mechanical Properties of Resin Transfer Molded Composites. In *Materials: Processing, Characterization and Modeling of Novel Nano-Engineered and Surface Engineered Materials, Proceedings of the ASME 2002 International Mechanical Engineering Congress and Exposition, New Orleans, LA, USA, 17–22 November 2002*; ASME: New York, NY, USA, 2002; Volume 2002, pp. 173–181. [CrossRef]
63. Sugiman, S.; Salman, S. Hygrothermal effects on tensile and fracture properties of epoxy filled with inorganic fillers having different reactivity to water. *J. Adhes. Sci. Technol.* **2019**, *33*, 691–714. [CrossRef]
64. Bordes, M.; Davies, P.; Cognard, J.Y.; Sohier, L.; Sauvant-Moynot, V.; Galy, J. Prediction of long term strength of adhesively bonded steel/epoxy joints in sea water. *Int. J. Adhes. Adhes.* **2009**, *29*, 595–608. [CrossRef]
65. Loh, W.K.; Crocombe, A.D.; Abdel Wahab, M.M.; Ashcroft, I.A. Modelling anomalous moisture uptake, swelling and thermalcharacteristics of a rubber toughened epoxy adhesive. *Int. J. Adhes. Adhes.* **2005**, *25*, 1–12. [CrossRef]
66. Scida, D.; Aboura, Z.; Benzeggagh, M. The effect of ageing on the damage events in woven-fibre composite materials under different loading conditions. *Compos. Sci. Technol.* **2002**, *62*, 551–557. [CrossRef]
67. Cândido, G.M.; Costa, M.L.; Rezende, M.C.; Almeida, S.F.M. Hygrothermal effects on quasi-isotropic carbon epoxy laminates with machined and molded edges. *Compos. Part B Eng.* **2008**, *39*, 490–496. [CrossRef]
68. Cao, Y.; Qian, X.; Liu, C.; Yang, J.; Xie, K.; Zhang, C. Controllable preparation of a novel epoxy/anhydride system with polyether-Polyester semi-interpenetrating structure and the excellent hydrothermal aging resistance properties. *Polym. Degrad. Stabil.* **2019**, *168*, 1–10. [CrossRef]
69. Wang, M.; Xu, X.; Ji, J.; Yang, Y.; Shen, J.; Ye, M. The hygrothermal aging process and mechanism of the novolac epoxy resin. *Compos. Part B Eng.* **2016**, *107*, 1–8. [CrossRef]
70. Guo, B.; Jia, D.; Fu, W.; Qiu, Q. Hygrothermal stability of dicyanate-novolac epoxy resin blends. *Polym. Degrad. Stabil.* **2003**, *79*, 521–528. [CrossRef]
71. Capiel, G.; Miccio, L.A.; Montemartini, P.E.; Schwartz, G.A. Water diffusion and hydrolysis effect on the structure and dynamics of epoxy-anhydride networks. *Polym. Degrad. Stabil.* **2017**, *143*, 57–63. [CrossRef]
72. El Yagoubi, J.; Lubineau, G.; Roger, F.; Verdu, J. A fully coupled diffusion-reaction scheme for moisture sorption-desorption in an anhydride-cured epoxy resin. *Polymer* **2012**, *53*, 5582–5595. [CrossRef]
73. Bréthous, R.; Colin, X.; Fayolle, B.; Gervais, M. Non-Fickian behavior of water absorption in an epoxy-amidoamine network. In Proceedings of the VIII International Conference on Times of Polymers and Composites, Naples, Italy, 19–23 June 2016; AIP Publishing: Melville, NY, USA, 2016; p. 020070. [CrossRef]
74. Pupure, L.; Doroudgarian, N.; Joffe, R. Moisture uptake and resulting mechanical response of biobased composites. I. constituents. *Polym. Compos.* **2013**, *35*, 1150–1159. [CrossRef]
75. Verge, P.; Toniazzo, V.; Ruch, D.; Bomfim, J.A. Unconventional plasticization threshold for a biobased bisphenol-A epoxy substitution candidate displaying improved adhesion and water-resistance. *Ind. Crops Prod.* **2014**, *55*, 180–186. [CrossRef]
76. Mannberg, P.; Nyström, B.; Joffe, R. Service life assessment and moisture influence on bio-based thermosetting resins. *J. Mater. Sci.* **2014**, *49*, 3687–3693. [CrossRef]
77. Núñez, L.; Villanueva, M.; Fraga, F.; Núñez, M.R. Influence of Water Absorption on the Mechanical Properties of DGEBA (n=0)/1, 2 DCH Epoxy System. *J. Appl. Polym. Sci.* **1999**, *74*, 353–358. [CrossRef]
78. Apicella, A.; Nicolais, L. Role of processing on the durability of epoxy composites in humid environments. *Ind. Eng. Chem. Prod. Res. Dev.* **1984**, *23*, 288–297. [CrossRef]
79. Suzuki, T.; Oki, Y.; Numajiri, M.; Miura, T.; Kondo, K. Free-volume characteristics and water absorption of novolac epoxy resins investigated by positron annihilation. *Polymer* **1996**, *37*, 3025–3030. [CrossRef]
80. Cadu, T.; Van Schoors, L.; Sicot, O.; Moscardelli, S.; Divet, L.; Fontaine, S. Cyclic hygrothermal ageing of flax fibers' bundles and unidirectional flax/epoxy composite. Are bio-based reinforced composites so sensitive? *Ind. Crops Prod.* **2019**, *141*, 1–12. [CrossRef]

81. Assarar, M.; Scida, D.; El Mahi, A.; Poilâne, C.; Ayad, R. Influence of water ageing on mechanical properties and damage events of two reinforced composite materials: Flax–fibres and glass–fibres. *Mater. Des.* **2011**, *32*, 788–795. [CrossRef]
82. Newman, R.H. Auto-accelerative water damage in an epoxy composite reinforced with plain-weave flax fabric. *Compos. Part A Appl. Sci. Manuf.* **2009**, *40*, 1615–1620. [CrossRef]
83. Scida, D.; Assarar, M.; Poilâne, C.; Ayad, R. Influence of hygrothermal ageing on the damage mechanisms of flax-fibre reinforced epoxy composite. *Compos. Part B Eng.* **2013**, *48*, 51–58. [CrossRef]
84. Yan, L.; Chouw, N. Effect of water, seawater and alkaline solution ageing on mechanical properties of flax fabric/epoxy composites used for civil engineering applications. *Construct. Build. Mater.* **2015**, *99*, 118–127. [CrossRef]
85. Perrier, A.; Touchard, F.; Chocinski-Arnault, L.; Mellier, D. Quantitative analysis by micro-CT of damage during tensile test in a woven hemp/epoxy composite after water ageing. *Compos. Part A Appl. Sci. Manuf.* **2017**, *102*, 18–27. [CrossRef]
86. Doroudgarian, N.; Pupure, L.; Joffe, R. Moisture uptake and resulting mechanical response of bio-based composites. II. Composites. *Polym. Compos.* **2015**, *36*, 1510–1519. [CrossRef]
87. Islam, M.S. The Influence of Fibre Processing and Treatments on Hemp Fibre/Epoxy and Hemp Fibre/PLA Composites. Ph.D. Thesis, University of Waikato, Hamilton, New Zealand, 2008.
88. Wan, Y.; Wang, Y.; Huang, Y.; Luo, H.; He, F.; Chen, G. Moisture absorption in a three-dimensional braided carbon/Kevlar/epoxy hybrid composite for orthopaedic usage and its influence on mechanical performance. *Compos. Part A Appl. Sci. Manuf.* **2006**, *37*, 1480–1484. [CrossRef]
89. Aronhime, M.T.; Neumann, S.; Marom, G. The anisotropic diffusion of water in Kevlar-epoxy composites. *J. Mater. Sci.* **1987**, *22*, 2435–2446. [CrossRef]
90. Piasecki, F. Résines Polyépoxydes Nanostructurées aux Propriétés d'Adhésion et à la Tenue au Vieillissement Améliorées. Ph.D. Thesis, Université de Bordeaux-I, Laboratoire de Chimie des Polymères Organiques, Bordeaux, France, 2013.
91. Akay, M.; Ah Mun, S.K.; Stanley, A. Influence of moisture on the thermal and mechanical properties of autoclaved and oven-cured Kevlar-49/epoxy laminates. *Compos. Sci. Technol.* **1997**, *57*, 565–571. [CrossRef]
92. Hahn, H.T.; Kim, K.S. Hygroscopic Effects in Aramid Fiber/Epoxy Composite. *J. Eng. Mater. Technol.* **1988**, *110*, 153–157. [CrossRef]
93. Sinchuk, Y.; Pannier, Y.; Antoranz-Gonzalez, R.; Gigliotti, M. Analysis of moisture diffusion induced stress in carbon/epoxy 3D textile composite materials with voids by μ-CT based Finite Element Models. *Compos. Struct.* **2019**, *212*, 561–570. [CrossRef]
94. Wan, Y.Z.; Wang, Y.L.; Cheng, G.X.; Han, K.Y. Three-dimensionally braided carbon fiber-epoxy composites, a new type of material for osteosynthesis devices. I. Mechanical properties and moisture absorption behavior. *J. Appl. Polym. Sci.* **2002**, *85*, 1031–1039. [CrossRef]
95. Yuan, Y.; Zhou, C.w. Meso-Scale Modeling to Characterize Moisture Absorption of 3D Woven Composite. *Appl. Compos. Mater.* **2016**, *23*, 719–738. [CrossRef]
96. Abacha, N.; Kubouchi, M.; Sakai, T.; Tsuda, K. Diffusion behavior of water and sulfuric acid in epoxy/organoclay nanocomposites. *J. Appl. Polym. Sci.* **2009**, *112*, 1021–1029. [CrossRef]
97. Dell'Anno, G.; Lees, R. Effect of water immersion on the interlaminar and flexural performance of lowcost liquid resin infused carbon fabric composites. *Compos. Part Eng.* **2012**, *43*, 1368–1372. [CrossRef]
98. Larbi, S.; Bensaada, R.; Bilek, A.; Djebali, S. Hygrothermal ageing effect on mechanical properties of FRP laminates. In Proceedings of the AIP 4th International Congress in Advances in Applied Physics and Materials Science, Fethiye, Turkey, 24–24 April 2015; AIP Publishing: Melville, NY, USA, 2015. [CrossRef]
99. Collings, T.; Stone, D. Hygrothermal effects in CFC laminates: Damaging effects of temperature, moisture and thermal spiking. *Compos. Struct.* **1985**, *3*, 341–378. [CrossRef]
100. Vanlandingham, M.R.; Eduljee, R.F.; Gillespie, J.W. Moisture diffusion in epoxy systems. *J. Appl. Polym. Sci.* **1999**, *71*, 787–798. [CrossRef]
101. Johncok, P.; Tudgey, G.F. Some Effects of Structure, Composition and Cure on the Water Absorption and Glass Transition Temperature of Amine-cured Epoxies. *Br. Polym. J.* **1986**, *18*, 292–302. [CrossRef]
102. Bellenger, V.; Verdu, J.; Morel, E. Structure-properties relationships for densely cross-linked epoxide-amine systems based on epoxide or amine mixtures. Part 2: Water absorption and diffusion. *J. Mater. Sci.* **1989**, *24*, 63–68. [CrossRef]
103. Xiao, G.; Shanahan, M. Swelling of DGEBA/DDA epoxy resin during hygrothermal ageing. *Polymer* **1998**, *39*, 3253–3260. [CrossRef]
104. Heman, M.B. Contribution à l'Etude des Interphases et de Leur Comportement au Vieillissement Hygrothermique dans les Systèmes à Matrice Thermodurcissable Renforcés de Fibres de Verre. Ph.D. Thesis, Université du Sud-Toulon-Var, Laboratoire Matériaux à Finalités Spécifiques, La Garde, France, 2008.
105. Xiao, G.; Shanahan, M. Irreversible effects of hygrothermal aging on DGEBA/DDA epoxy resin. *J. Appl. Polym. Sci.* **1998**, *69*, 363–369. [CrossRef]
106. Shirrell, C.D.; Halpin, J. Moisture absorption and desorption in epoxy composite laminates. In *Proceedings of the Composite Materials: Testing and Design*; Davis West, J., Ed.; ASTM International: West Conshohocken, PA, USA, 1977; pp. 514–528.
107. Martin, R. *Ageing of Composites. Composites Science and Engineering*; Woodhead Publishing Series: Cambridge, UK, 2008.
108. Lefebvre, D.; Dillard, D.; Ward, T. A model for the diffusion of moisture in adhesive joints. Part I: Equations governing diffusion. *J. Adhes.* **1989**, *27*, 1–18. [CrossRef]
109. Crank, J. *The Mathematics of Diffusion*; Clarendon Press: Oxford, UK, 1975.

110. Weitsman, Y.J. Diffusion models. In *Fluid Effects in Polymers and Polymeric Composites*; Springer: New York, NY, USA, 2012; pp. 69–94. [CrossRef]
111. Placette, M.D.; Fan, X. A Dual Stage Model of Anomalous Moisture Diffusion and Desorption in Epoxy Mold Compounds. In Proceedings of the 12th International Conference on Thermal, Mechanical and Multiphysics Simulation and Experiments in Micro-Electronics and Micro-Systems EuroSimE, Linz, Austria, 18–20 April 2011; IEEE: Linz, Autriche, 2011; pp. 1–8.
112. Alston, S.; Korkees, F.; Arnold, C. Finite element modelling of moisture uptake in carbone fibre/epoxy composites: A multi-scale approach. In Proceedings of the ECCM15 Proceedings; ESCM: 15th European Conference on Composite Materials, Venice, Italy, 24–28 June 2012.
113. Gurtin, M.E.; Yatomi, C. On a Model for Two Phase Diffusion in Composite Materials. *J. Compos. Mater.* **1978**, *13*, 126–130. [CrossRef]
114. Chambers, J.M.; Cleveland, W.S.; Kleiner, B.; Tukey, P.A. *Graphical Methods for Data Analysis*; Chapman and Hall/CRC: Boca Raton, FL, USA, 2018.
115. Ugarte, M.D.; Militino, A.F.; Arnholt, A.T. *Probability and Statistics with R*; CRC Press: Boca Raton, FL, USA, 2008.
116. Cornillon, P.A.; Husson, F.; Jégou, N.; Matzner-Lober, E.; Josse, J.; Guyader, A.; Rouvière, L.; Kloareg, J. *Statistiques avec R; Pratique de la Statistique*; Presses Universitaires de Rennes: Paris, France, 2012.
117. Van Krevelen, D.W. *Properties of Polymers: Their Correlation with Chemical Structure Their Numerical Estimation and Prediction from Additive Group Contributions*, 4th ed.; Elsevier: Amsterdam, The Netherlands, 2009.
118. Verdu, J. *Action de l'Eau sur les Plastiques*; Techniques de l'Ingénieur: Paris, France, 2000; pp. 1–11.
119. Morel, E.; Bellenger, V.; Verdu, J. *Relations Structure-Hydrophilie des Réticultats Epoxyde-Amine*; Pluralis Ed: Paris, France, 1984; pp. 597–614.
120. McKague, E.L.; Reynolds, J.D.; Halkias, J.E. Swelling and glass transition relations for epoxy matrix material in humid environments. *J. Appl. Polym. Sci.* **1978**, *22*, 1643–1654. [CrossRef]
121. Cotugno, S.; Larobina, D.; Mensitieri, G.; Musto, P.; Ragosta, G. A novel spectroscopic approach to investigate transport processes in polymers: The case of water-epoxy system. *Polymer* **2001**, *42*, 6431–6438. [CrossRef]
122. Karad, S.K.; Jones, F.R. Mechanisms of moisture absorption by cyanate ester modified epoxy resin matrices: The clustering of water molecules. *Polymer* **2005**, *46*, 2732–2738. [CrossRef]
123. Fuller, R.T.; Fornes, R.E.; Memory, J.D. NMR study of water absorbed by epoxy resin. *J. Appl. Polym. Sci.* **1979**, *23*, 1871–1874. [CrossRef]
124. Pascault, J.P.; Sautereau, H.; Verdu, J.; Williams, R.J.J. *Thermosetting Polymers*; Marcel Dekker: New York, Ny, USA, 2002.
125. Bouvet, G. Relations Entre Microstructure et Propriétés Physico-Chimiques et Mécaniques de Revêtements Epoxy Modèles. Ph.D. Thesis, Université de La Rochelle, Laboratoire des Sciences de l'Ingénieur pour l'Environnement, Paris, France, 2014.
126. Apicella, A.; Nicolais, L.; de Cataldis, C. Characterization of the morphological fine structure of commercial thermosetting resins through hygrothermal experiments. *Adv. Polym. Sci.* **2005**, *66*, 189–207.
127. Bellenger, V.; Decelle, J.; Huet, N. Ageing of a carbon epoxy composite for aeronautic applications. *Compos. Part Eng.* **2005**, *36*, 189–194. [CrossRef]
128. Alam, P.; Robert, C.; Ó Brádaigh, C.M. Tidal turbine blade composites—A review on the effects of hygrothermal aging on the properties of CFRP. *Compos. Part Eng.* **2018**, *149*, 248–259. [CrossRef]
129. Adamson, M.J. Thermal expansion and swelling of cured epoxy resin used in graphite/epoxy composite materials. *J. Mater. Sci.* **1980**, *15*, 1736–1745. [CrossRef]
130. Al-Maharma, A.Y.; Al-Huniti, N. Critical review of the parameters affecting the effectiveness of moisture absorption treatments used for natural composites. *J. Compos. Sci.* **2019**, *3*, 27. [CrossRef]
131. Azwa, Z.; Yousif, B.; Manalo, A.; Karunasena, W. A review on the degradability of polymeric composites based on natural fibres. *Mater. Des.* **2013**, *47*, 424–442. [CrossRef]
132. Hamid, M.R.Y.; Ab Ghani, M.H.; Ahmad, S. Effect of antioxidants and fire retardants as mineral fillers on the physical and mechanical properties of high loading hybrid biocomposites reinforced with rice husks and sawdust. *Ind. Crop. Prod.* **2012**, *40*, 96–102. [CrossRef]
133. Xie, Y.; Hill, C.A.; Xiao, Z.; Militz, H.; Mai, C. Silane coupling agents used for natural fiber/polymer composites: A review. *Compos. Part Appl. Sci. Manuf.* **2010**, *41*, 806–819. [CrossRef]
134. Tang, X.; Whitcomb, J.D.; Li, Y.; Sue, H.J. Micromechanics modeling of moisture diffusion in woven composites. *Compos. Sci. Technol.* **2005**, *65*, 817–826. [CrossRef]
135. Almudaihesh, F.; Holford, K.; Pullin, R.; Eaton, M. The influence of water absorption on unidirectional and 2D woven CFRP composites and their mechanical performance. *Compos. Part Eng.* **2020**, *182*, 107626. [CrossRef]
136. Wan, Y.; Wang, Y.; Huang, Y.; He, B.; Han, K. Hygrothermal aging behaviour of VARTMed three-dimensional braided carbon-epoxy composites under external stresses. *Compos. Part Appl. Sci. Manuf.* **2005**, *36*, 1102–1109. [CrossRef]
137. Gollins, K.; Chiu, J.; Delale, F.; Liaw, B.; Gursel, A. Comparison of Manufacturing Techniques Subject to High Speed Impact. In Proceedings of the ASME International Mechanical Engineering Congress and Exposition, Montreal, QC, Canada, 14–20 November 2014; Volume 46583, p. V009T12A019.
138. Bhatt, A.T.; Gohil, P.P.; Chaudhary, V. Primary manufacturing processes for fiber reinforced composites: History, development & future research trends. In *Proceedings of the IOP Conference Series: Materials Science and Engineering*; IOP Publishing: Bristol, UK, 2018; Volume 330, p. 012107.

139. Park, S.Y.; Choi, C.H.; Choi, W.J.; Hwang, S.S. A Comparison of the Properties of Carbon Fiber Epoxy Composites Produced by Non-autoclave with Vacuum Bag Only Prepreg and Autoclave Process. *Appl. Compos. Mater.* **2019**, *26*, 187–204. [CrossRef]
140. Wolter, N.; Beber, V.C.; Yokan, C.M.; Storz, C.; Mayer, B.; Koschek, K. The effects of manufacturing processes on the physical and mechanical properties of basalt fibre reinforced polybenzoxazine. *Compos. Commun.* **2021**, *24*, 100646. [CrossRef]
141. Hopfenberg, H.; Stannett, V. The diffusion and sorption of gases and vapours in glassy polymers. In *The Physics of Glassy Polymers*; Springer: Berlin/Heidelberg, Germany, 1973; pp. 504–547.
142. Barrer, R.M.; Barrie, J.A.; Slater, J. Sorption and diffusion in ethyl cellulose. Part III. Comparison between ethyl cellulose and rubber. *J. Polym. Sci.* **1958**, *27*, 177–197. [CrossRef]
143. Flory, P.J. *Principles of Polymer Chemistry*; Cornell University Press: Cornell, UK, 1953.
144. Fick, A. Über diffusion. *Ann. Phys. Hig. Poggendroff* **1855**, *170*, 59–86. [CrossRef]
145. Obeid, H. Durabilité de Composites à Matrice Thermoplastique Sous Chargement hygromécanique: Etude Multi-Physique et Multiéchelle des Relations Microstructure-Propriétés—états Mécaniques. Ph.D. Thesis, Université Bretagne-Loire, Institut de Recherche en Génie Civil et Mécanique (GeM), Nantes, France, 2016.
146. Loos, A.C.; Springer, G.S. Moisture Absorption of Graphite-Epoxy Composites Immersed in Liquids and in Humid Air. *J. Compos. Mater.* **1979**, *13*, 131–147. [CrossRef]
147. Zeng, W.; Du, Y.; Xue, Y.; Frisch, H.L. Solubility parameters. In *Physical Properties of Polymers Handbook*, 2nd ed.; Mark, J.E., Ed.; Springer: New York, NY, USA, 2006; pp. 289–305.
148. Charlas, M. Étude et Durabilité de Solutions de Packaging Polymère de Module d'Electronique de Puissance à Application Aéronautique. Ph.D. Thesis, Université de Pau et des Pays de l'Adour, Institut des Sciences Analytiques et de Physico-Chimie pour l'Environnement et les Matériaux, Pau, France, 2009.
149. Hansen, C.M. *Hansen Solubility Parameters: A User's Handbook*, 2nd ed.; CRC Press: Boca Raton, FL, USA, 2007.
150. Jolliffe, I.T. *Principal Component Analysis*; Springer: New York, NY, USA, 1986.
151. Meglen, R.R. Examining large databases: A chemometric approach using principal component analysis. *J. Chemom.* **1991**, *5*, 163–179. [CrossRef]
152. Jolliffe, I.T.; Cadima, J. Principal component analysis: A review and recent developments. *Philos. Trans. R. Soc. Math. Phys. Eng. Sci.* **2016**, *374*, 1–16. [CrossRef] [PubMed]
153. Villar Montoya, M. Procédé de Soudage Laser de Polymères Haute Performance: Etablissement des Relations entre les Paramètres du Procédé, la Structure et la Morphologie du Polymère et les Propriétés Mécaniques de l'Assemblage. Ph.D. Thesis, Institut National Polytechnique de Toulouse, Laboratoire Génie de Production (INP-ENIT), Paris, France, 2018.
154. Husson, F.; Lê, S.; Pagès, J. *Exploratory Multivariate Analysis by Example Using R. Computer Science & Data Analysis*; Chapman Hall/CRC Press: Boca Raton, FL, USA, 2011.
155. Lê, S.; Josse, J.; Husson, F. FactoMineR: An R Package for Multivariate Analysis. *J. Stat. Softw.* **2008**, *25*, 1–18. [CrossRef]
156. Dunteman, G.H. *Principal Components Analysis*; Sage Publications: Thousand Oaks, CA, USA, 1989; p. 69
157. Kassambara, A. *Practical Guide To Principal Component Methods in R; Vol. Multivariate Analysis II, Statistical Tools for High-throughput Data Analysis (STHDA)*; Sage Publications: Thousand Oaks, CA, USA, 2017.
158. Peres-Neto, P.R.; Jackson, D.A.; Somers, K.M. How many principal components? Stopping rules for determining the number of non-trivial axes revisited. *Comput. Stat. Data Anal.* **2005**, *49*, 974–997. [CrossRef]
159. Simar, A.; Gigliotti, M.; Grandidier, J.C.; Ammar-Khodja, I. Decoupling of water and oxygen diffusion phenomena in order to prove the occurrence of thermo-oxidation during hygrothermal aging of thermosetting resins for RTM composite applications. *J. Mater. Sci.* **2018**, *53*, 11855–11872. [CrossRef]
160. Farrar, N.R.; Ashbee, K.H.G. Destruction of epoxy resins and of glass-fibre-reinforced epoxy resins by diffused water. *J. Phys. Appl. Phys.* **1978**, *11*, 1009–1015. [CrossRef]
161. Fedors, R.F. Osmotic effects in water absorption by polymers. *Polymer* **1980**, *21*, 207–212. [CrossRef]
162. Gautier, L.; Mortaigne, B.; Bellenger, V.; Verdu, J. Osmotic cracking nucleation in hydrothermal-aged polyester matrix. *Polymer* **2000**, *41*, 2481–2490. [CrossRef]
163. Colin, X.; Verdu, J.; Rabaud, B. Stabilizer Thickness Profiles in Polyethylene Pipes Transporting Drinking Water Disinfected by Bleach. *Polym. Eng. Sci.* **2011**, *51*, 1539–1549. [CrossRef]
164. Moisan, J.Y. Diffusion des additifs du polyéthylène I: Influence de la nature du diffusant. *Eur. Polym. J.* **1980**, *16*, 979–987. [CrossRef]
165. Abdessalem, A.; Tamboura, S.; Fitoussi, J.; Ben Daly, H.; Tcharkhtchi, A. Bi-phasic water diffusion in sheet molding compound composite. *J. Appl. Polym. Sci.* **2020**, *137*, 1–12. [CrossRef]
166. Berthé, V.; Ferry, L.; Bénézet, J.; Bergeret, A. Ageing of different biodegradable polyesters blends mechanical and hygrothermal behavior. *Polym. Degrad. Stab.* **2010**, *95*, 262–269. [CrossRef]
167. Gillet, C.; Nassiet, V.; Poncin-Epaillard, F.; Hassoune-Rhabbour, B.; Tchalla, T. Chemical behaviour of water absorption in a carbon/epoxy 3D woven composite. In *Macromolecular Symposia, Proceedings of the10th International Conference on Times of Polymers and Composites, Ischia, Italy, 30 April 2022*; Wiley Online Library: Hoboken, NJ, USA, 2022.
168. Gillet, C.; Hassoune-Rhabbour, B.; Poncin-Epaillard, F.; Tchalla, T.; Nassiet, V. Contributions of atmospheric plasma treatment on a hygrothermal aged carbon/epoxy 3D woven composite material. *Polym. Degrad. Stab.* **2022**, *202*, 110023. [CrossRef]

169. Guloglu, G.E.; Hamidi, Y.K.; Altan, M.C. Fast recovery of non-fickian moisture absorption parameters for polymers and polymer composites. *Polym. Eng. Sci.* **2017**, *57*, 921–931. [CrossRef]
170. Cocaud, J.; Célino, A.; Fréour, S.; Jacquemin, F. What about the relevance of the diffusion parameters identified in the case of incomplete Fickian and non-Fickian kinetics? *J. Compos. Mater.* **2019**, *53*, 1555–1565. [CrossRef]